AD-A144 469 DEFLAGRATION TO SHOCK TO DETONATION TRANSITION OF ENERGETIC PROPELLANTS..(U) ILLINOIS UNIV AT URBANA DEPT OF MECHANICAL AND INDUSTRIAL ENG.. H KRIER ET AL. 1/1

UNCLASSIFIED JUL 84 UILU-ENG-84-4006 AFOSR-TR-84-0634 F/G 21/8.2 NL

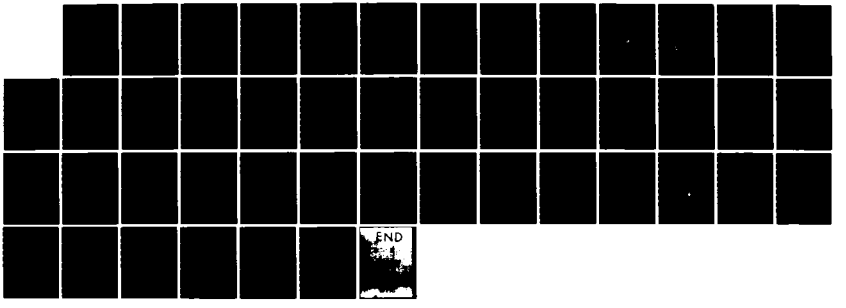

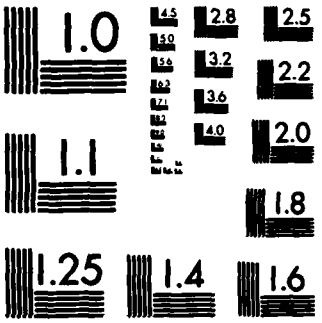

MICROCOPY RESOLUTION TEST CHART
NATIONAL BUREAU OF STANDARDS-1963-A

AFOSR-TR- 84-0634

University of Illinois at Urbana-Champaign
Urbana, IL 61801

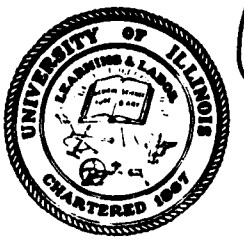

(4)

Annual Report UILU ENG 84-4006

AD-A144 469

DEFLAGRATION TO SHOCK TO DETONATION TRANSITION OF ENERGETIC PROPELLANTS

Annual Technical Report
Grant AFOSR 81-0145

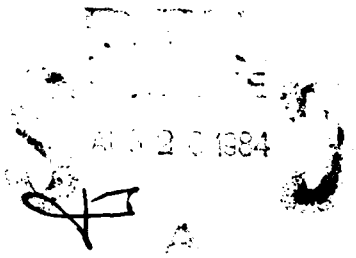

July 1984

Approved for public release;
distribution unlimited.

Copy available to DTIC does not permit fully legible reproduction

DTIC FILE COPY

84 08 17 072

DISCLAIMER NOTICE

THIS DOCUMENT IS BEST QUALITY PRACTICABLE. THE COPY FURNISHED TO DTIC CONTAINED A SIGNIFICANT NUMBER OF PAGES WHICH DO NOT REPRODUCE LEGIBLY.

Annual Report*

DEFLAGRATION TO SHOCK TO DETONATION TRANSITION OF ENERGETIC PROPELLANTS

Prepared by:

Herman Krier, Principal Investigator(*)
P. Barry Butler and Chris Cudak, Graduate Research Assistants

Department of Mechanical and Industrial Engineering
144 Mechanical Engineering Building
1206 West Green Street
University of Illinois at Urbana-Champaign
Urbana, IL 61801

Prepared for:

Air Force Office of Scientific Research
Aerospace Sciences Directorate: Bldg. 410
Bolling Air Force Base, DC 20332
Program Manager: Dr. Henry R. Radoski

For Research Performed under

(*) Grant AFOSR 81-0145

During Period 1 June 1983 through 30 May 1984

AIR FORCE OFFICE OF SCIENTIFIC RESEARCH (AFSC)
NOTICE OF TRANSMITTAL TO DTIC
This technical report has been reviewed and is approved for public release IAW AFR 190-12 (7b).
Distribution is unlimited.
MATTHEW J. KERPER
Chief, Technical Information Division

* Approved for Public Release: Distribution Unlimited, Grant AFOSR 81-0145
July 1984

REPORT DOCUMENTATION PAGE

READ INSTRUCTIONS BEFORE COMPLETING FORM

1. REPORT NUMBER: AFOSR-TR- 84-0631
2. GOVT ACCESSION NO.: AD-A144469
3. RECIPIENT'S CATALOG NUMBER:

4. TITLE (and Subtitle): DEFLAGRATION TO SHOCK TO DETONATION TRANSITION IN ENERGETIC PROPELLANTS
5. TYPE OF REPORT & PERIOD COVERED: Annual Report July 1984
6. PERFORMING ORG. REPORT NUMBER: UILU ENG 84-4006

7. AUTHOR(s): Herman Krier, P. Barry Butler, Chris Cudak
8. CONTRACT OR GRANT NUMBER(s): AFOSR 81-0145

9. PERFORMING ORGANIZATION NAME AND ADDRESS: University of Illinois at Urbana-Champaign, Department of Mechanical and Industrial Engineer., Urbana, IL 61801
10. PROGRAM ELEMENT, PROJECT, TASK AREA & WORK UNIT NUMBERS: 61102F 2308/A1

11. CONTROLLING OFFICE NAME AND ADDRESS: Air Force Office of Scientific Research/NP, Building 410; ATTN: Henry R. Radoski, Bolling Air Force Base, DC 20332
12. REPORT DATE: July 1984
13. NUMBER OF PAGES: 44

14. MONITORING AGENCY NAME & ADDRESS (if different from Controlling Office):
15. SECURITY CLASS. (of this report): UNCLASSIFIED
15a. DECLASSIFICATION/DOWNGRADING SCHEDULE:

16. DISTRIBUTION STATEMENT (of this Report): Approved for public release; distribution unlimited

17. DISTRIBUTION STATEMENT (of the abstract entered in Block 20, if different from Report):

18. SUPPLEMENTARY NOTES:

19. KEY WORDS (Continue on reverse side if necessary and identify by block number):
Detonation physics
DDT (Deflagration to Detonation Transition)
Porous Explosives and Propellants

20. ABSTRACT (Continue on reverse side if necessary and identify by block number):
It is well known that explosive-based propellants are susceptible to detonation from the controlled deflagration mode of combustion. In certain instances (i.e. when the propellant/explosive is fragmented) the likelihood of a catastrophic event is greater. Fragment size, gas permeability through the packed bed, chemical decomposition rate and product gas confinement all play an important role in determining whether a convective deflagration wave will make a transition to a steady state detonation wave. In some instances a confined

zone of granulated propellant adjacent to a zone of cast propellant can provide a rapid enough pressure-rise rate to shock initiate the cast material. If the cast propellant has voids, the detonation will initiate at some location ahead of the granulated bed/cast material interface.

This report is a summary of the research activities that focus on the analysis and modeling of the physics of such highly transient flows. The report includes (as Appendices) two technical papers prepared during the past year on the topic of DSDT (Deflagration to Shock to Detonation Transition).

Abstract

It is well known that explosive-based propellants are susceptible to detonation from the controlled deflagration mode of combustion. In certain instances (i.e. when the propellant/explosive is fragmented) the likelihood of a catastrophic event is greater. Fragment size, gas permeability through the packed bed, chemical decomposition rate and product gas confinement all play an important role in determining whether a convective deflagration wave will make a transition to a steady state detonation wave. In some instances a confined zone of granulated propellant adjacent to a zone of cast propellant can provide a rapid enough pressure-rise rate to shock initiate the cast material. If the cast propellant has voids, the detonation will initiate at some location ahead of the granulated bed/cast material interface.

This report is a summary of the research activities that focus on the analysis and modeling of the physics of such highly transient flows. The report includes (as Appendices) two technical papers prepared during the past year on the topic of DSDT (Deflagration to Shock to Detonation Transition).

DTIC COPY INSPECTED

A-1

1. Introduction

The probability of a detonation occurring in a solid propellant rocket motor greatly increases when secondary high-explosives (HE) are used as constituents in the propellant mixture. Octogen (HMX) and cyclotrimethylene trinitramine (RDX) are the most commonly used nitramine HE in todays propellant formulations. By increasing the explosive content of solid propellants the overall performance of the system increases as well as the sensitivity to detonation by shock initiation. Since the early 1970's laboratories at both the Air Force and Navy have researched and tested solid propellant formulations containing secondary explosives such a RDX and HMX. As will be discussed briefly, a detonation hazard exists when burning these high-energy propellants, which is not present during the combustion of "standard" composite and composite-double base propellants.

By burning more energetic propellant constituents the specific impulse and thus overall performance of a solid rocket motor can be increased. However, one disadvantage which comes with using these explosive-based propellant mixtures is the hazard of Deflagration to Shock to Detonation Transition (DSDT). A DSDT event is when a controlled subsonic deflagration wave makes a transition to a high order detonation. The result is total destruction of the motor assembly.

In the literature (reviewed in Appendices A and B) this process is more commonly referred to as Deflagration to Detonation Transition (DDT). Our research group at Illinois coined the description DSDT in order to emphasize that Shock to Detonation Transition (SDT) is the final step in the process. Both terms, DDT and DSDT, will be used interchangeably throughout the text.

2. DSDT in Granulated Solid Propellant

In the papers included as Appendices A and B, three different flow processes have been identified as DDT (DSDT). Two are real possibilities in the rocket motor environment and the third is only possible when using a high order cast explosive under extreme confinement. (It is also unlikely that a solid rocket motor would be cast with pure explosive.) But studying this third scenerio provides basic information on detonation initiation mechanisms. This section has been included in order to differentiate between the three cases and provide the reader with a basic understanding of the sequence of event leading to detonation in each of them.

Case 1

What will be referred to as "DDT-Case 1" involves a transition to detonation occurring within a bed of totally porous, granulated propellant. Consider the rocket motor shown in Fig. 1. For illustration purposes, a center-burning configuration is shown. It is hypothesized that the normal burning process of the cast solid propellant in the rocket motor is disturbed by an abnormality such as a crack (see Fig. 1) in the propellant grain [1,2], thus providing the granulated region. Figure 2 shows an enlargement of the granulated region. The fracture could be the result of a handling accident during shipment or nozzle failure during operation. Because of the increased surface-to-volume ratio of the resulting propellant fragments, product gas generation increases beyond the level necessary for steady-state motor operation. That is, the mass produced in the chamber exceeds the mass leaving the nozzle. Pressure gradients, developed as a result of localized burning, drive the hot product gases into the cracks developed in the upstream propellant. As a consequence of this unsteady flow process, convective heat

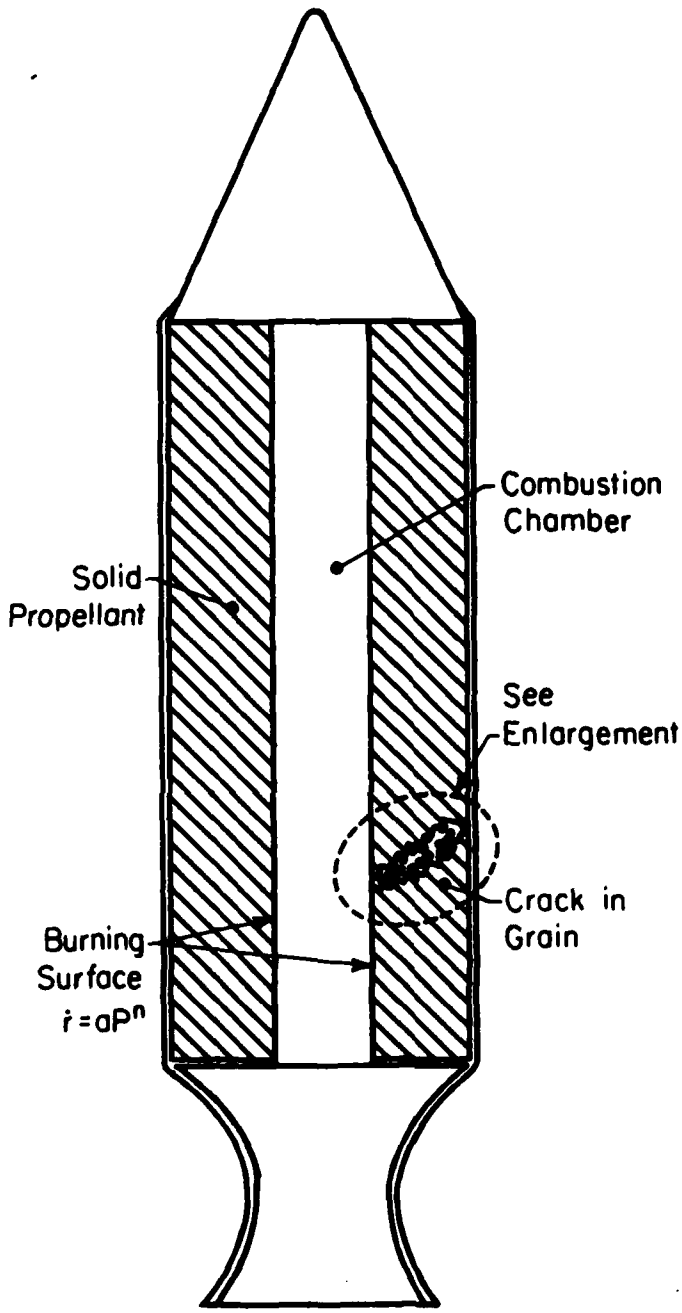

DSDT HAZARD IN ROCKET MOTOR

Fig. 1 Sketch of solid propellant rocket motor with cracked grain.

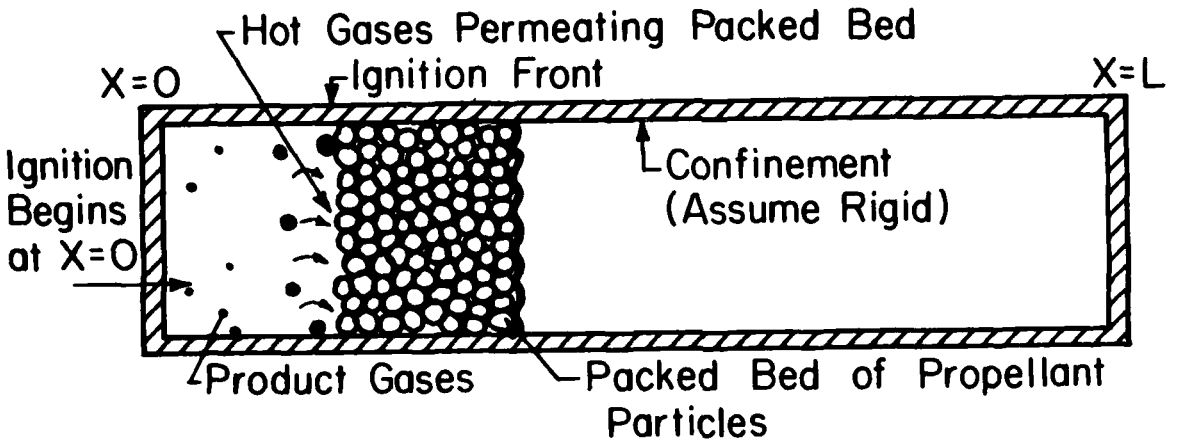

DSDT IN PACKED BED

Fig. 2 Enlargement of granulated bed formed in rocket grain (See Fig. 1).

transfer from the hot gas to the unreacted propellant will ignite more of the upstream propellant particles. Under certain circumstances the process can be self-propagating. That is, as the propellant decomposes, the pressure wave strengthens, which in time leads to the ignition of more propellant. This accelerated convective burning can eventually lead to shock compression of the upstream propellant and a possible detonation transition.

Figure 3 illustrates the general form of a pressure-distance profile once the steady state detonation solution is obtained. For illustration purposes, the profile is superimposed on a sketch of a granulated bed. The shock front is followed by a narrow reaction zone (not to scale in Fig. 3) which is followed by an expansion zone consisting of all product gases. Appendix A, "Analysis of Deflagration to Shock to Detonation Transition (DSDT) in Porous Energetic Solid Propellants," by Butler and Krier, is a detailed study of the "DDT-Case 1" scenerio. The reader should consult Appendix A for a discussion on the governing equations and predicted DSDT results.

Case 2

A second DDT scenerio, "DDT-Case 2," involves the rapid local pressurization in a region of granulated propellant as the necessary impetus to shock initiate an adjacent region of cast but void-containing propellant. This is illustrated in Fig. 4. The cast material (Zone 1) can contain 'blind' pores, but is assumed to be impermeable to the flow of hot gases form the granular zone (Zone 2). This implies that, unlike the first DDT scenerio discussed, only stress waves can be transmitted upstream of the reaction zone. A second characteristic of Case 2 is that the length of the granular bed is less than the detonation run-up length, ℓ_{CJ}. The important point here is that although the granular bed is shorter than the critical detonation run-

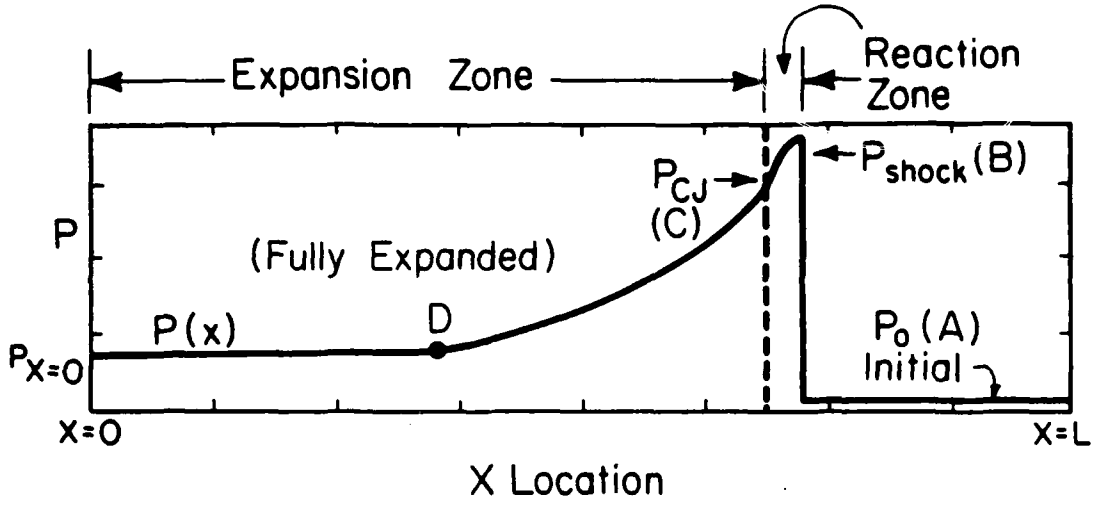

Fig. 3 Schematic of Packed Bed after Transition to Detonation. Ignition region has collapsed to a thin zone and is followed by an all gas expansion zone.

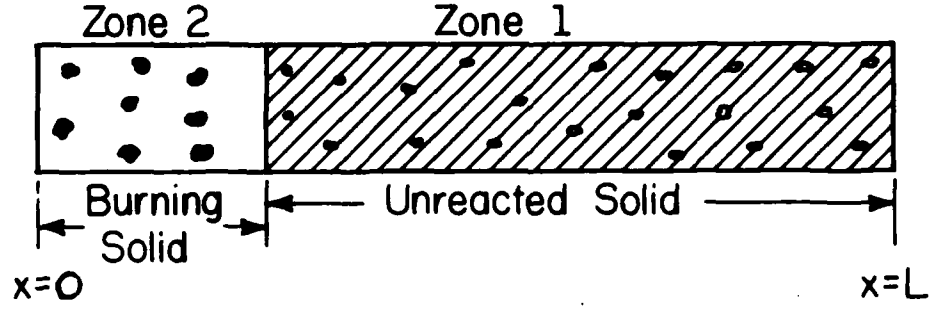

Fig. 4 Sketch of granulated bed/cast bed configuration (Case 2) for DSDT.

up length, the impermeable material can still detonate. DDT-Case 2 was studied in detail by Cudak, Krier and Butler [3] which is attached as Appendix B.

Figure 5 shows the pressure-time profiles acting on the granular bed/cast solid interface for various propellant sizes [3]. As shown in the figure, the pressure-rise rate is strongly dependent upon the grain size. The larger the particle size, the slower the pressure-rise rate. The cases studied in Ref. 3 had rise-time of $0 \leq t^* < 30\mu s$. This pressure-rise function is used as a boundary condition for the unsteady flow analysis upstream of the interface.

The governing equations defining stress wave propagation and subsequent detonation upstream of the interface are the usual flow equations for one-dimensional flow in a continuous medium. In a Lagrangian formulation, one writes,

$$v_t = vu_x \tag{1}$$

$$u_t = -vP_x \tag{2}$$

and

$$e_t = -Pv_t + Q \tag{3}$$

where v is specific volume, u particle velocity, P pressure, e specific internal energy, and Q chemical energy release rate. The subscripts 'x' and 't' represent partial derivatives with respect to space and time respectively. Here, one is conserving the mixture properties, i.e. both solid and gas.

In addition to the conservation equations (Eqs. 1-3), an equation of state, $P = P(e,v)$, (Eq.4), and the reciprocal caloric equation of state $e = e(v,T)$, (Eq. 5), are needed for both the solid and product gas phases. Finally, a stress-void volume pore collapse relation

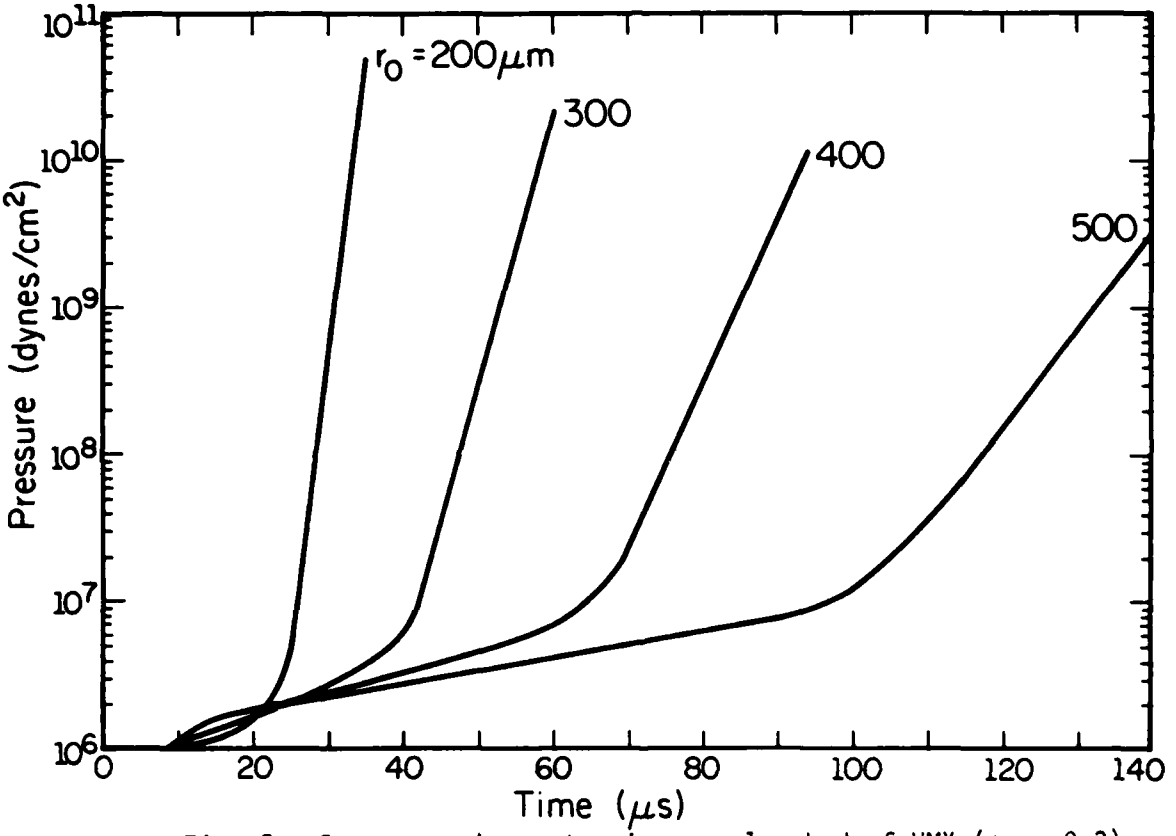

Fig. 5 Pressure-rise rates in granular bed of HMX (ϕ_0 = 0.3).

$$P = P(\alpha) \tag{6}$$

and energy partition equation

$$E_T = E_s + E_g \tag{7}$$

are required to complete the mathematical description of the flow behavior prior to reaction. In Eq. 7, E represents total energy, subscript 's' the solid phase and subscript 'g' the gas phase. Appendix B provides additional information concerning these equations.

Once reaction commences, a chemical decomposition rate

$$\frac{dW}{dt} = f(W,E^*,T^*) \tag{8}$$

is also needed to define the complete problem. Here, W represents an undecomposed mass fraction, E* an activation energy and T* represents a reaction temperature.

Experimental work [4] has shown that material samples containing voids and density irregularities will undergo shock to detonation transitions at much lower shock pressures than a homogeneous sample of the same material. Shock waves not strong enough to raise the bulk temperature of the material above the thermal explosion level are distorted by the density discontinuities of the porous material and subsequently superheat the material in these localized regions above the explosion level. Following this, the material reacts and strenghtens the leading shock wave which causes the transition to a detonation. These "hot spots", as they are referred to, are an initiating mechanism in porous reactive material [5].

The emphasis of the work cited in Appendix B was to show that ramp-loading porous materials to relatively low peak stresses can lead to detonation. In most cases, the bed detonated at a location downstream of the stress loaded boundary and an energy sustaining retonation wave was predicted to travel back towards the interface.

Figure 6 presents the pressure (stress wave) build-up history in a reactive solid with blind voids (α = 1.117), being pressurized to 2 GPA at a linear rate, taking 10 μsec.

In each portion of Figure 6 [parts (a) - (j)] we show the predicted pressure (stress) at the fixed time (shown in the upper left hand corner of the figures). Note, even as early as 8 μsec the material has been compressed by several millimeters, as evidenced by the 'gap' in the p - x variation near x = 0. At t = 16 μsec a steepend shock is clearly seen at x = 3.4 cm. At 18 μsec a detonation wave is predicted to begin traveling both forward and rearward.

Within another microsecond these oppositely-traveling reactive shocks are almost several centimeters apart, since the predicted detonation and retonation waves move at speeds of 8.3 and 8.7 mm/μsec, respectively. The retonation reflects from the front wall (interface) and a more complicated pressure distribution is shown in Figs. 6(h), 6(i) and 6(j).

The calculations shown in Figs. 6(a) - 6(j) considered an explosive (HMX) with an energy of 6.84 Mjoule/kg having a porosity of 10.5% (α = 1.1176). The material of this density, according to thermodynamic-equilibrium calculations is predicted to detonate at a C-J pressure of 27.9 GPa. Note that our transient flow calculations predicted an eventual steady C-J pressure for the detonation to be 27 GPa, a very good agreement.

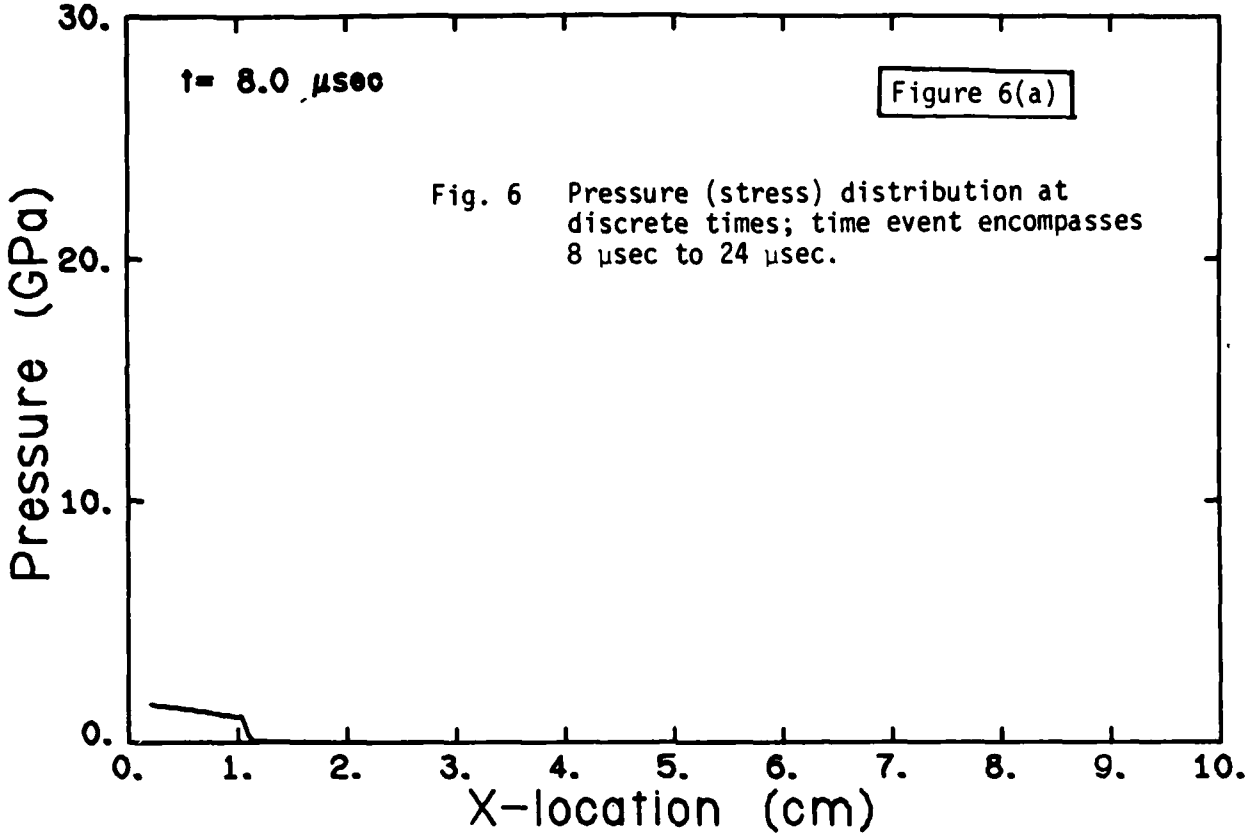

Fig. 6 Pressure (stress) distribution at discrete times; time event encompasses 8 μsec to 24 μsec.

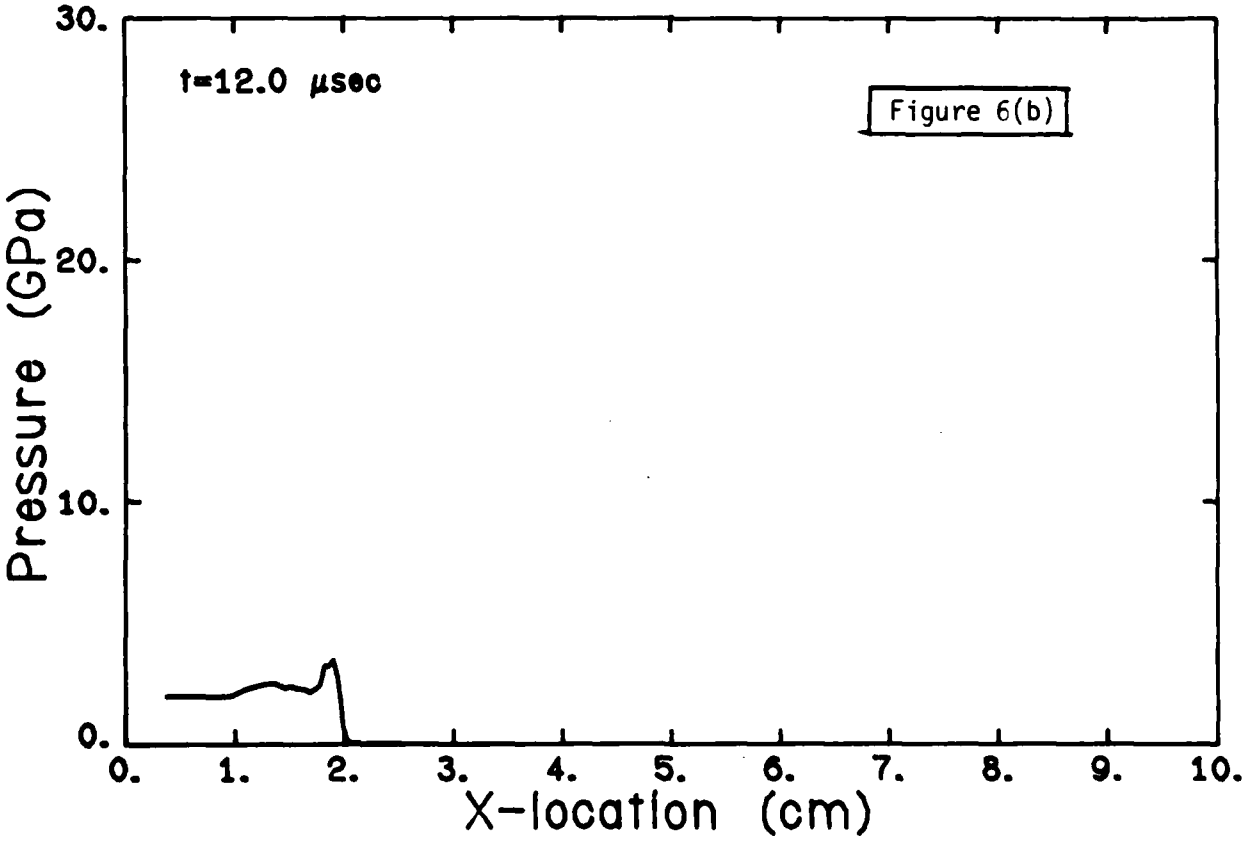

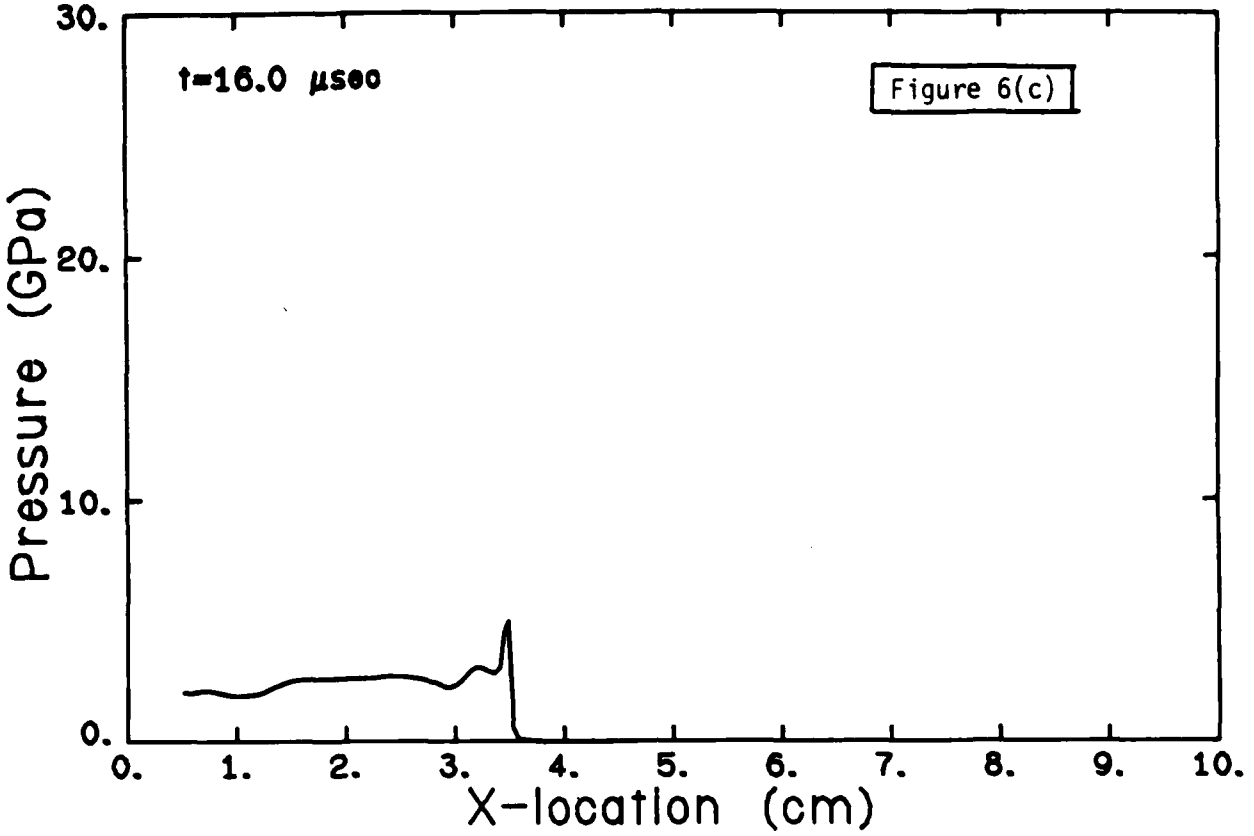
t=16.0 μsec
Figure 6(c)
Pressure (GPa)
30.
20.
10.
0.
0. 1. 2. 3. 4. 5. 6. 7. 8. 9. 10.
X-location (cm)

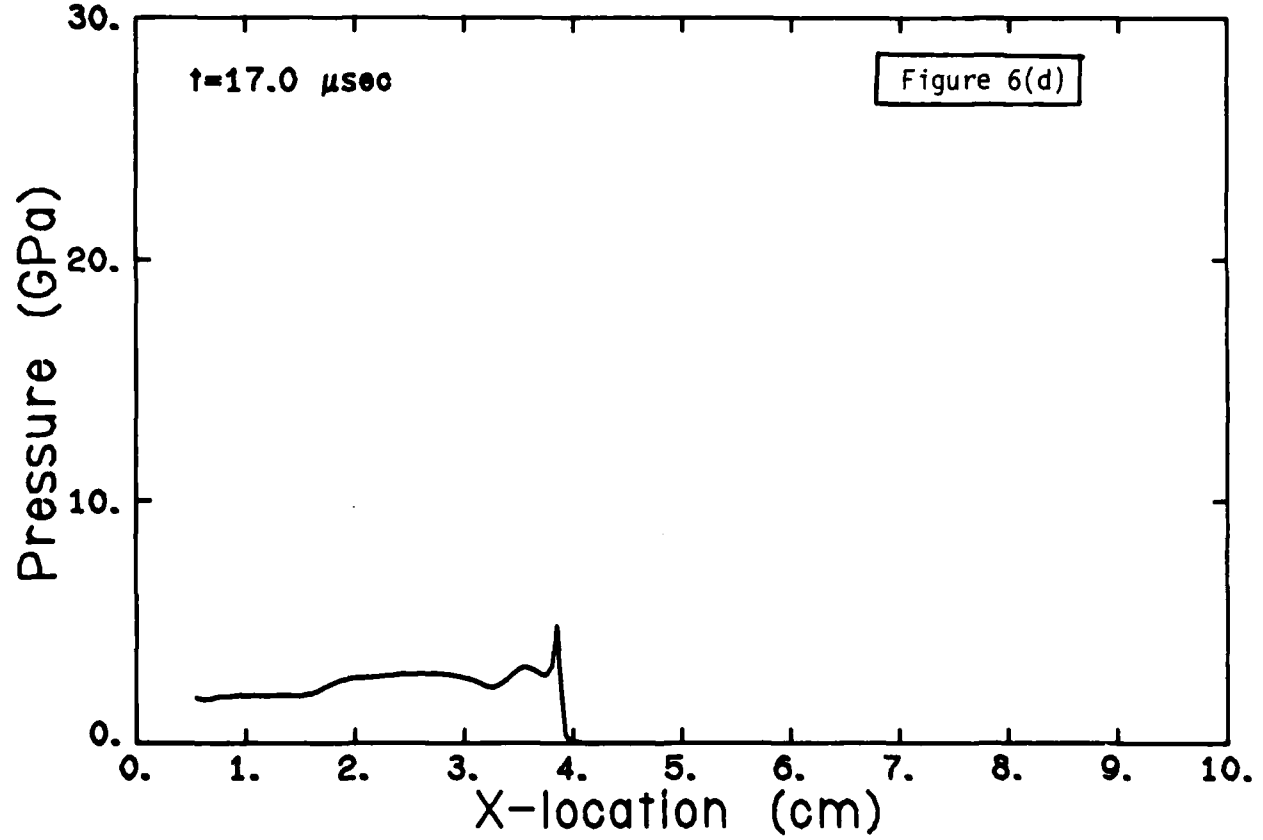
t=17.0 μsec
Figure 6(d)
Pressure (GPa)
30.
20.
10.
0.
0. 1. 2. 3. 4. 5. 6. 7. 8. 9. 10.
X-location (cm)

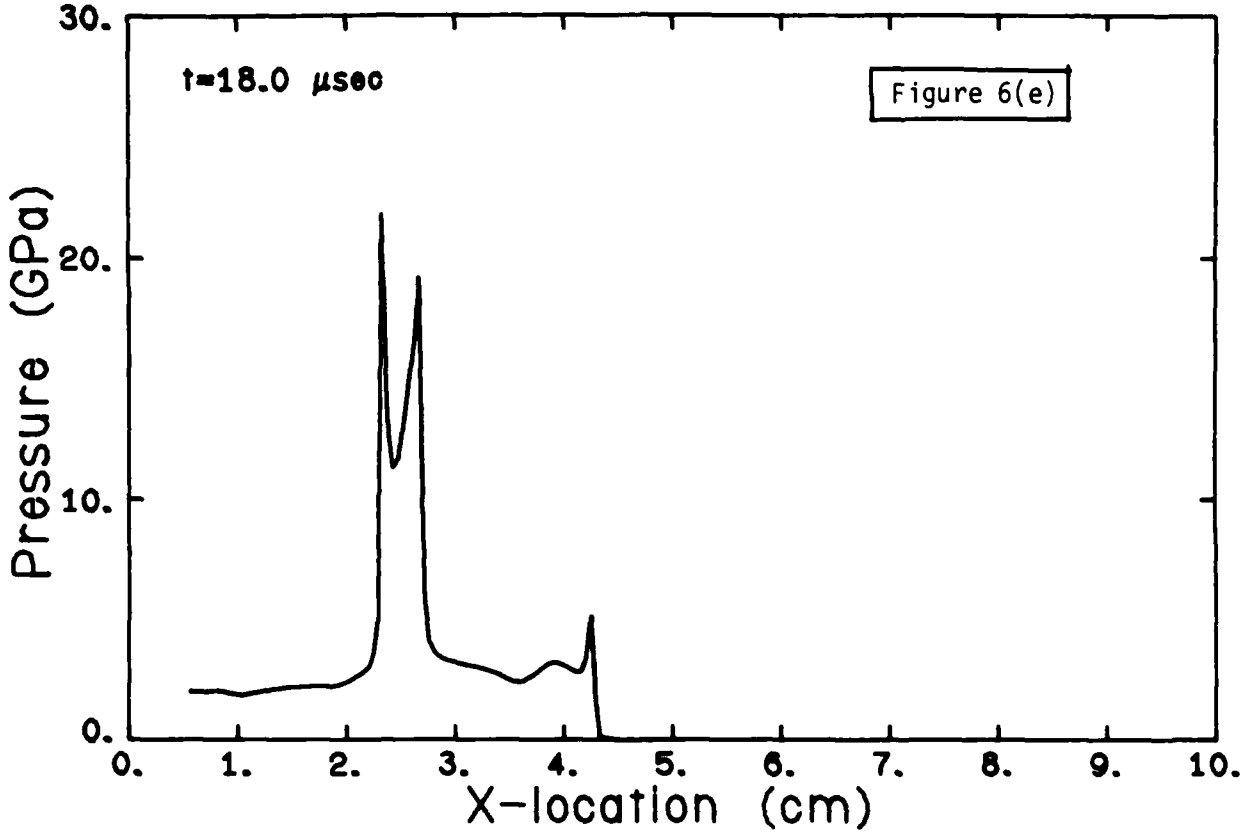
t=18.0 μsec
Figure 6(e)
Pressure (GPa)
30.
20.
10.
0.
0. 1. 2. 3. 4. 5. 6. 7. 8. 9. 10.
X-location (cm)

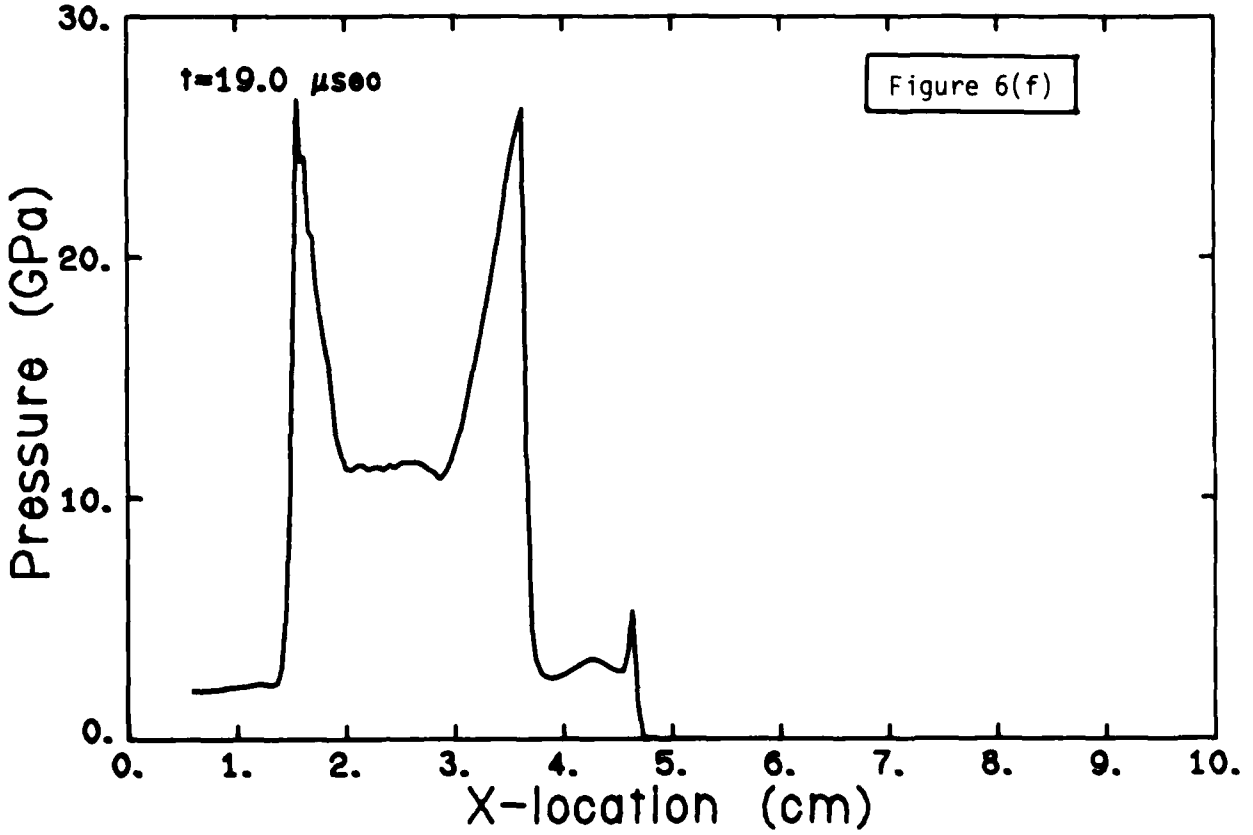
t=19.0 μsec
Figure 6(f)
Pressure (GPa)
30.
20.
10.
0.
0. 1. 2. 3. 4. 5. 6. 7. 8. 9. 10.
X-location (cm)

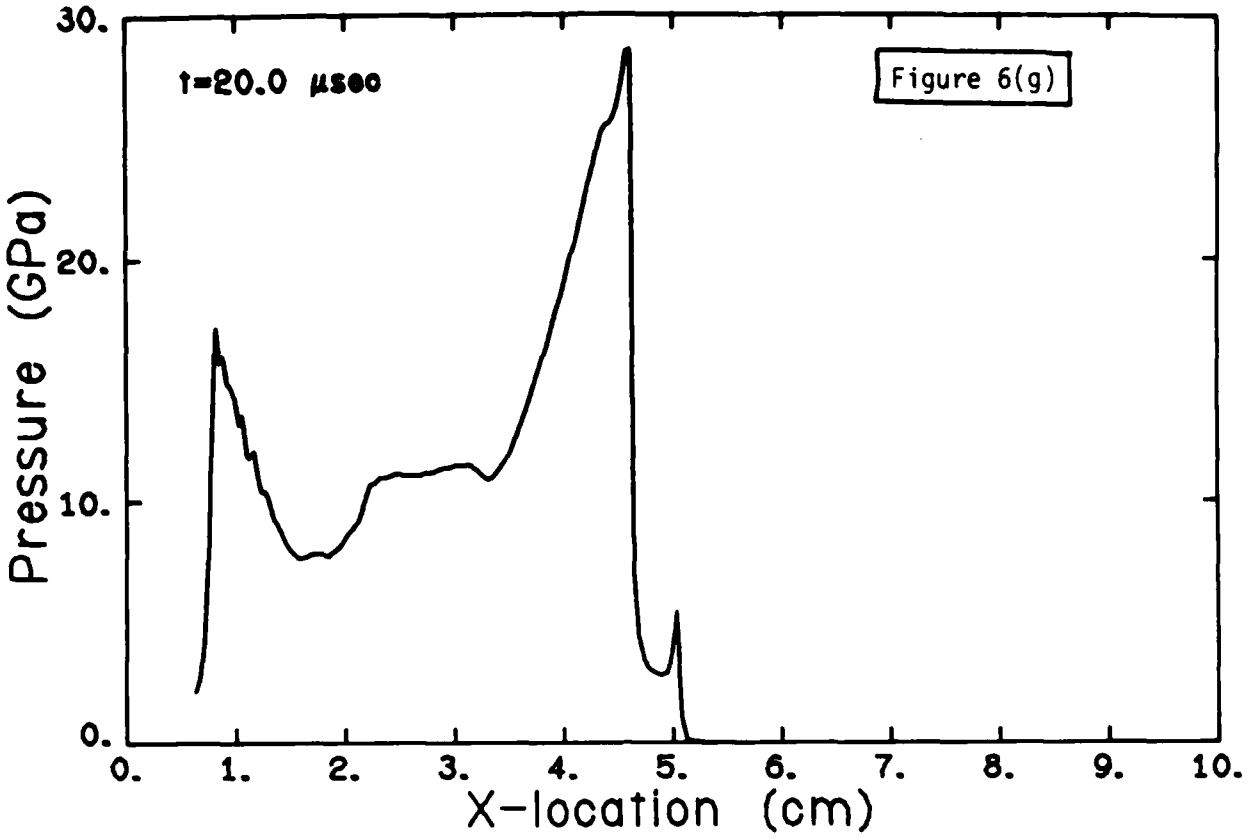
t=20.0 μsec
Figure 6(g)
Pressure (GPa)
30.
20.
10.
0.
0. 1. 2. 3. 4. 5. 6. 7. 8. 9. 10.
X-location (cm)

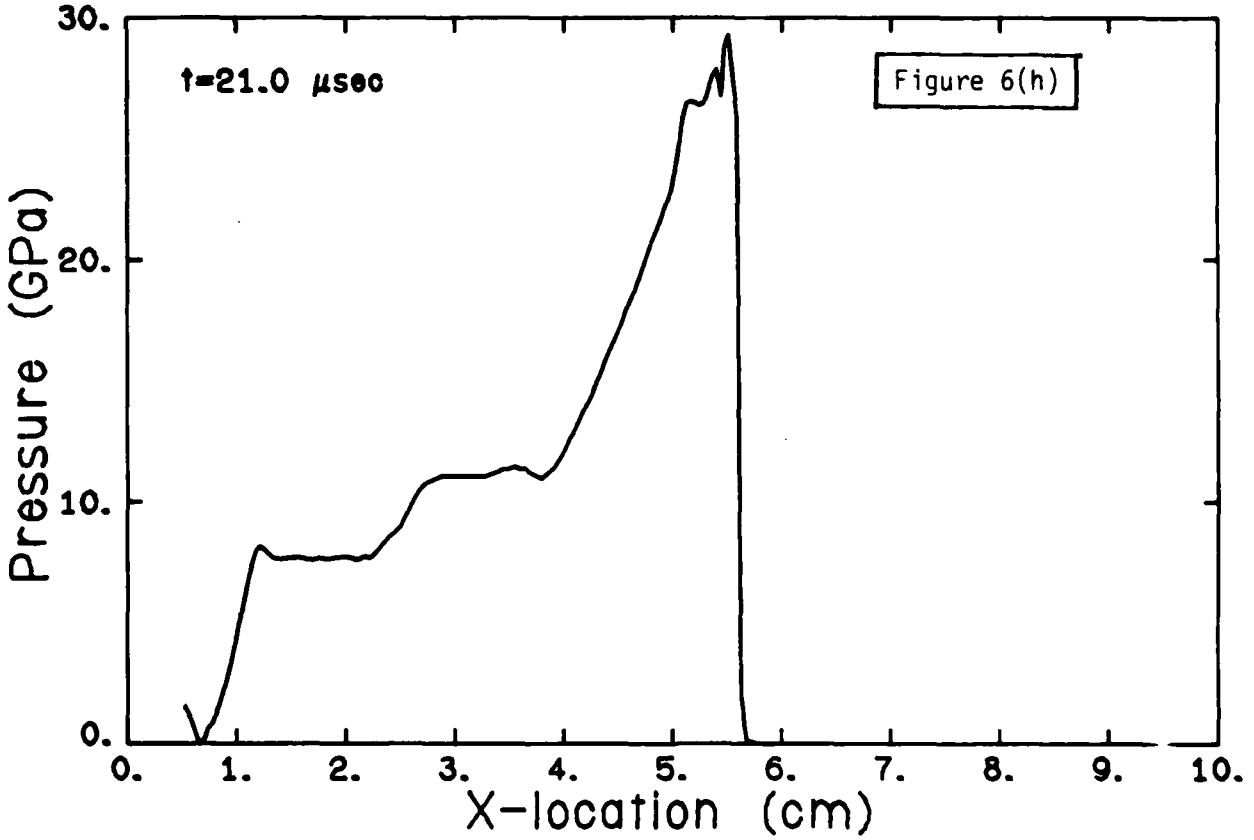
t=21.0 μsec
Figure 6(h)
Pressure (GPa)
30.
20.
10.
0.
0. 1. 2. 3. 4. 5. 6. 7. 8. 9. 10.
X-location (cm)

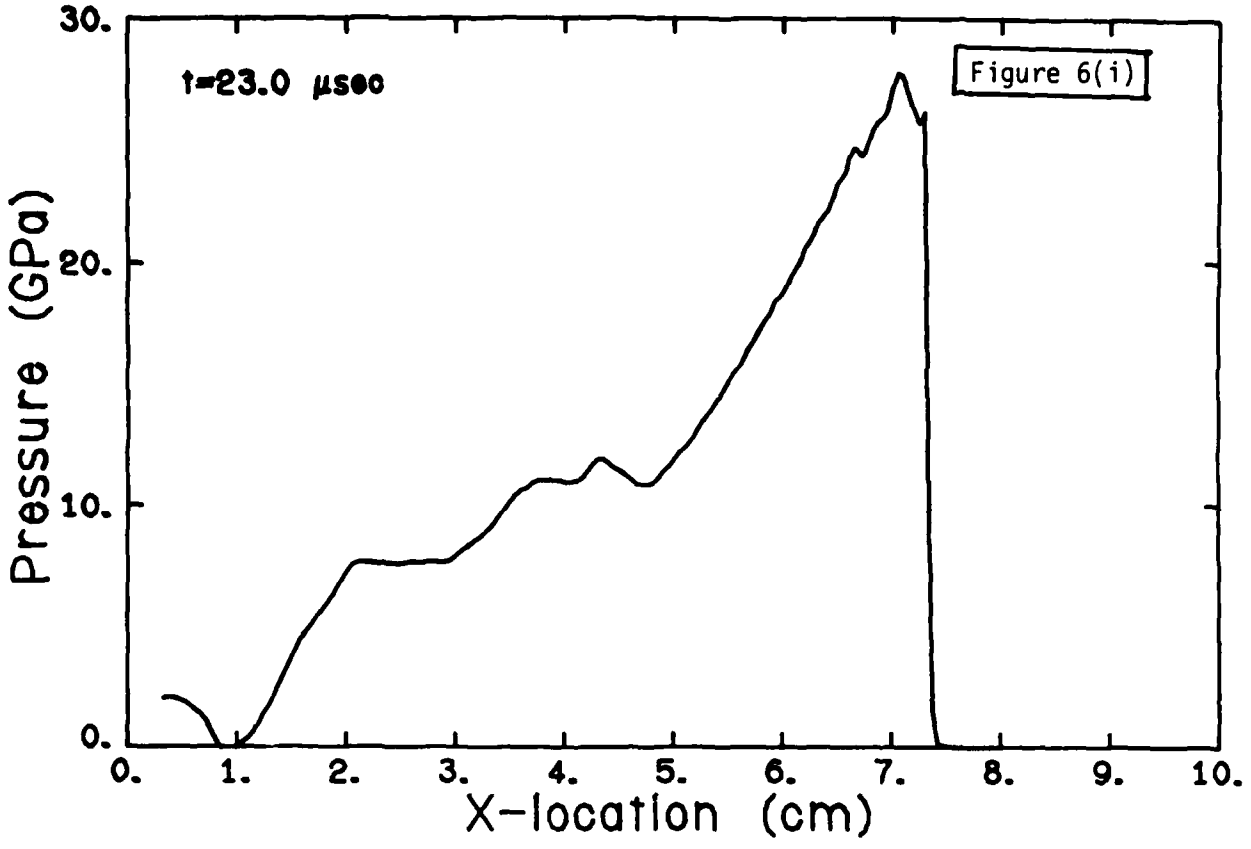
t=23.0 μsec
Figure 6(i)
Pressure (GPa)
30.
20.
10.
0.
0. 1. 2. 3. 4. 5. 6. 7. 8. 9. 10.
X-location (cm)

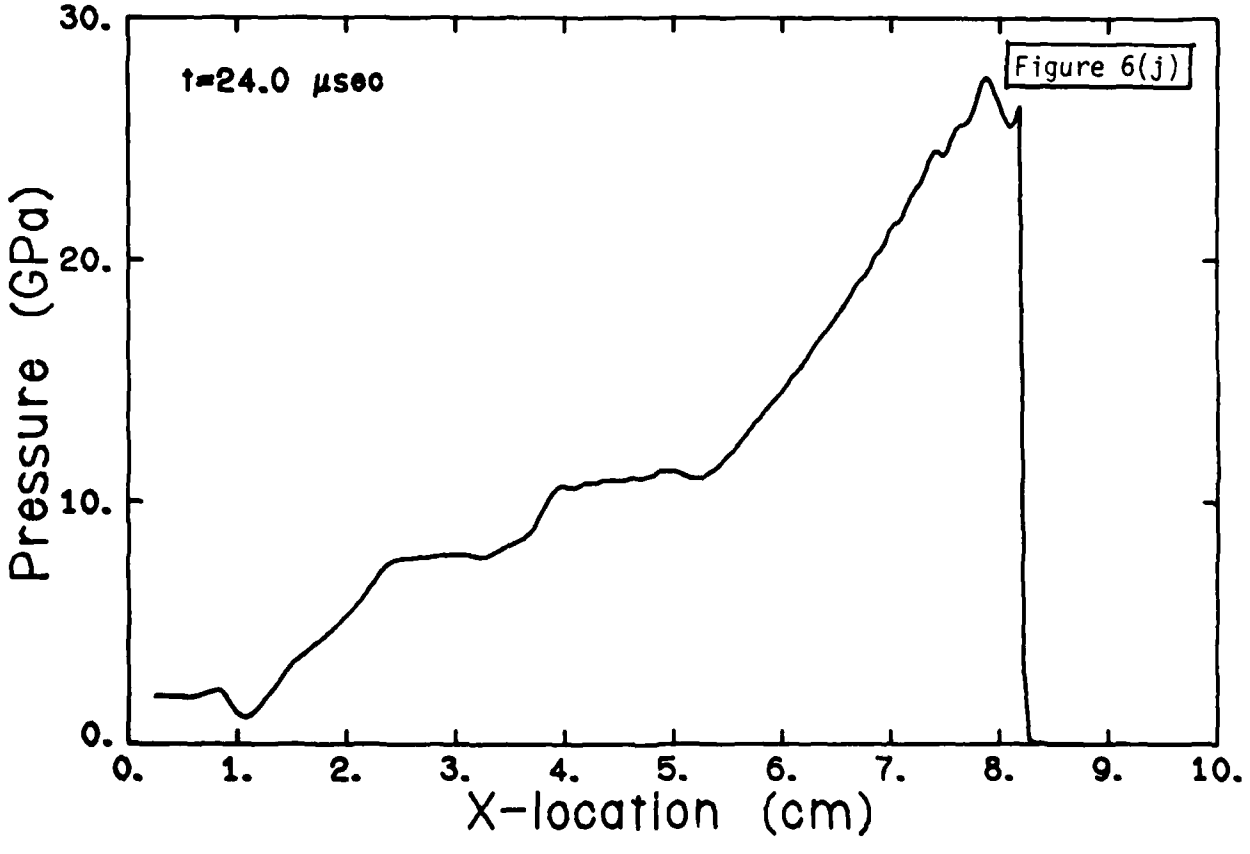
t=24.0 μsec
Figure 6(j)
Pressure (GPa)
30.
20.
10.
0.
0. 1. 2. 3. 4. 5. 6. 7. 8. 9. 10.
X-location (cm)

Figure 7 presents the locus of the stress wave (x-t diagram), shown as the dotted curve. At 17.8 μsec, at a location of 2.43 cm, a detonation (and retonation) is predicted. The slope in the x - t plane is, of course, the reaction front speed, and it is predicted to be 8.3 mm/μsec for the detonation, and 8.8 mm/μsec for the returning detonation (retonation), which travels into a pre-compressed (higher density) explosive.

Appendix B shows more results and provides details of the analysis. It is clear that our analysis is pertinent to the detonation physics responsible for DSDT is porous explosives. Of course, additional work is in order, since the sensitivity of the many assumptions on the predicted detonation run-up length has yet to be determined. For example, the variation in chemical activation energy during the rapid reaction process that supports the detonation can have a significant effect in the predicted run-up lengths.

Case 3

In both DSDT processes described above, the transition to detonation was the result of convective burning in a packed bed of reactive particles. In Case 1 the detonation transition occurred within the granulated bed and in Case 2 the detonation occurred in a cast, porous material upstream of the granulated bed. Nevertheless, in both cases the rapid pressurization rate due to the reacting fragmented bed provided the driving force necessary to shock initiate the material upstream. The third type of DDT discussed in the literature, "DDT-Case 3," results from end-burning (conductive combustion) a confined cast explosive (Fig. 8) which is impermeable to the flow of hot product gases. Although the manner in which the deflagration wave traverses the explosives is different from the first two cases, the end result (steady detonation wave) is the same.

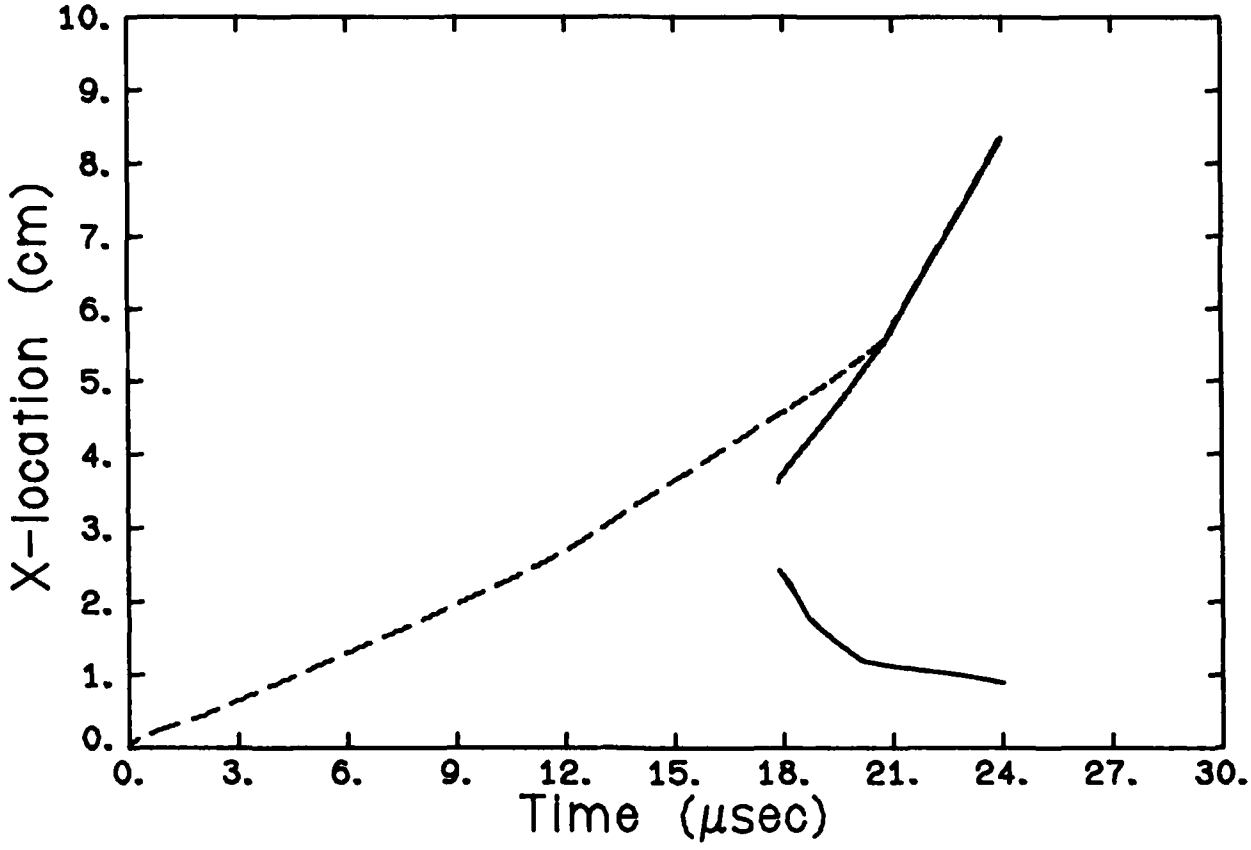

Fig. 7 Locus of stress front (dashed line) and the detonation and retonation front (solid line) for pressure history shown in Figures 6(a)-6(j).

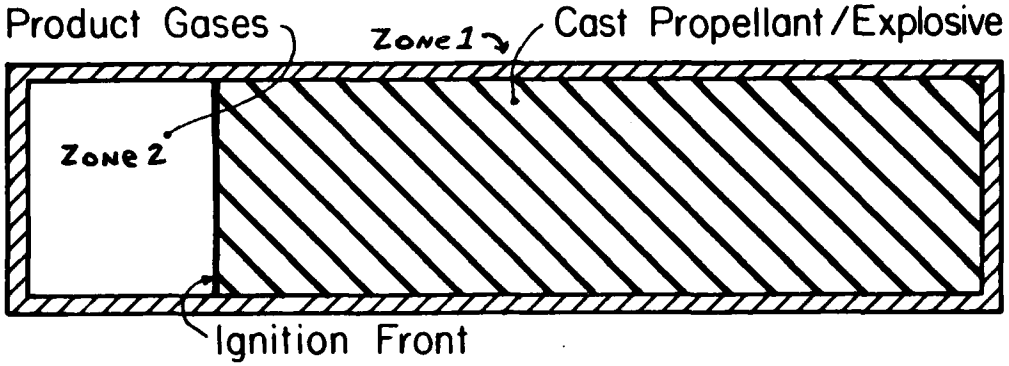

Fig. 8 Configuration of confined solid (impermeable) explosive end burning and causing pressure (stress) waves to propagate into the material.

Figure 8 is an illustration of the test configuration used in this type of DDT experiment. Here, the region labeled 'Zone 1' is a cast, voidless explosive and 'Zone 2' is occupied by the product gases generated in the propellant combustion. The sequence of events for this DDT begins with the thermal ignition of the explosive at the location x=0. This is then followed by the pressurization of the gas volume, (Zone 2), increased regression rate (dx/dt) of the burning material, stressing of the unreacted solid, shock formation ahead of the ignition front and eventual transition to detonation at the location of the upstream shock front formation. The driving force provided by the confined gases in Zone 2 is analogous to a moving piston with a prescribed velocity-time profile acting on the x=0 boundary, continually increasing the stress level in Zone 1. Although Case 3 has been shown to be a viable method for obtaining DDT in cast explosives, it will not cause DDT in cast propellants. Very simply, conductive combustion alone will not provide a rapid enough pressure-rise rate to shock initiate cast propellant.

1.3 Conclusions

In the work presented here and in our papers attached as Appendices, we have identified three different ways in which DSDT can occur in a solid rocket motor which has been damaged. The first two (Cases 1 and 2) are real possibilities in actual motors and the third is highly unlikely. Case 3 requires a perfect, voidless high energy reactive solid, in order to undergo a transition to detonation to the bulk material heating by rapid shock compression.

In Appendix A we showed that DDT can occur when a confined, but granular bed of high-energy, high reaction rate material is ignited at one end. The transient build up to detonation was only possible because of the convective

heat transfer mechanism from the hot gas to the unreacted propellant, early in the process. This DDT process was identified as DDT-Case 1.

DDT-Case 2, highlighted in Appendix B, occurs when the pressure-rise rate from a bed of granular propellant drives an adjacent porous cast material to detonation. As shown in Appendix B, this can occur at relatively low stress levels in the cast material.

References

1. Butler, P. B., M. L. Lembeck, and H. Krier, "Modeling of Shock Development and Transition to Detonation Initiated by Burning in Porous Propellant Beds," Combustion and Flame 46, (1982), 75-93.

2. Bernecker, R. R., "The DDT Process for High Energy Propellants," AGARD Conference Preprint No. 367, Paper No. 14, Lisse, The Netherlands, (1984).

3. Cudak, C. A., P. B. Butler, and H. Krier, "Transition to Detonation from Rapid-Compression (Ramp-Waves) Generated in a Burning Porous Bed," Presented at the 1984 JANNAF Propulsion Systems Hazards Meeting; APG, MD (June 1984).

4. Dick, J. J., "Measurement of the Shock Initiation Sensitivity of Low Density HMX," Combustion and Flame 54, (1983), 121-129.

5. Hayes, D. B., "Shock Induced Hot-Spot Formation and Subsequent Decomposition in Granular, Porous, Hexanitrostiblene Explosive," Detonation Physics Symposium, Minsk, Russia, (1981).

APPENDIX A: Paper to be published in NATO-AGARD Proceedings on Missle Hazards (1984).

ANALYSIS OF DEFLAGRATION TO SHOCK TO DETONATION TRANSITION (DSDT) IN POROUS ENERGETIC SOLID PROPELLANTS

P. Barry Butler and Herman Krier
Department of Mechanical and Industrial Engineering
University of Illinois at Urbana-Champaign
144 Mechanical Engineering Building
1206 West Green Street
Urbana, Illinois 61801
U.S.A.

SUMMARY

It is well known that explosive-based propellants are susceptible to detonation from the controlled deflagration mode of combustion. In certain instances (i.e. when the propellant/explosive is fragmented) the likelihood of a catastrophic event is greater. Fragment size, gas permeability through the packed bed, chemical decomposition rate and product gas confinement all play an important role in determining whether a convective deflagration wave will make a transition to a steady state detonation wave. The work presented here represents an effort to analyze and numerically model the governing equations defining such a transient two-phase reactive flow process. Computer generated results will be presented showing the development of a steady state detonation wave from an accelerating deflagration wave.

LIST OF SYMBOLS

b	burning rate coefficient
D	detonation velocity
$\vec{D}$	interphase viscous force
e	specific internal energy
E_{chem}	chemical energy of propellant
E_T	total energy
E	energy source (Eq. 7c, 8c)
f	drag coefficient (Eq. 14)
h_{pg}	convective heat transfer coefficient
k_g	thermal conductivity of gas
M_g	momentum source term (Eq. 7a, 8a)
n	burning rate index
p	pressure
Pr	Prantl number
$\dot{Q}$	interphase heat transfer rate
r	particle radius
$\dot{r}$	linear regression rate
Re	Reynolds number
R	gas constant
S	mass source (Eq. 7a, 8a)
t	time
T	temperature
u	velocity
v	specific volume
V	volume
x	distance
α	total volume/solid volume
Γ	mass generation rate
Γ'	Gruneisen parameter
η	covolume
ρ	density
ϕ	gas volume/total volume
μ_g	gas viscosity

Subscripts

1	partial gas phase
2	partial solid phase
g	gas phase
s	solid phase
HS	Hugoniot reference curve
CJ	Chapman-Jouguet
o	initial

INTRODUCTION

By burning more energetic propellant constituents such as the secondary explosives cyclic-trimethylenetrinintremene (RDX) and octogen (HMX) the specific impulse and thus overall performance of a solid rocket motor can be greatly increased. However, one disadvantage which comes with using these explosive-based propellant mixtures is the hazard of Deflagration to Shock to Detonation Transition (DSDT). A DSDT event is when a controlled subsonic deflagration wave makes a transition to a high-order detonation. The result is usually total destruction of the motor assembly. In a rocket motor the DSDT is usually associated with propellant fragmentation prior to the event. Although an actual motor has never been instrumented in fine enough detail to describe every event leading up to a DSDT, researchers have hypothesized what the sequence of pre-DSDT events might be.

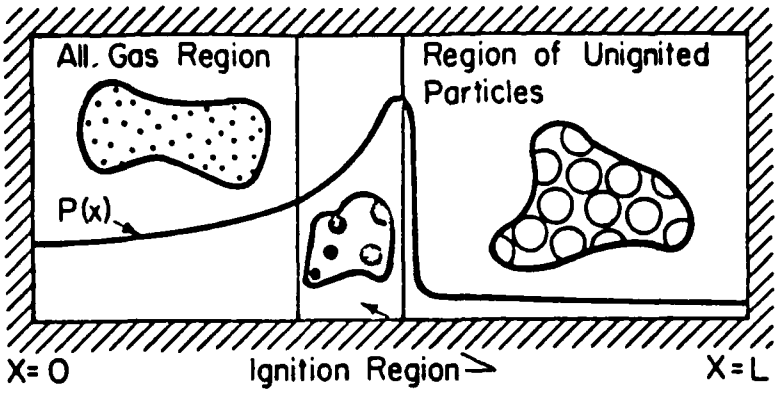

Fig. 1 Schematic of Packed Bed after Transition to Detonation. Ignition Region has Collapsed to a Thin Zone and is Followed by an all Gas Region.

As stated above, the first step in the DSDT process appears to be fragmentation of the grain. This can be the result of a handling accident during shipment or a nozzle failure during operation. Because of the increased surface-to-volume ratio of the resulting fragments, product gas generation increases beyond the level necessary for steady-state motor operation. That is, the mass produced in the chamber exceeds the mass leaving the nozzle. Pressure gradients, developed as a result of the localized burning, drive the hot product gases into the cracks developed in the upstream propellant. As a consequence of this flow process, convective heat transfer from the hot gas to the unreacted propellant will ignite more of the grain particles. The accelerated convective burning can eventually lead to shock compression of the upstream propellant and eventual detonation. Figure 1 is an illustration of a packed bed once the transition has occurred.

Due to the obvious hazard and complexity of the detonation transition process, there are limited experimental data available to verify the proposed model describing this dynamic event. It is nevertheless appropriate at this point to discuss and reference some of the experimental work on DSDT prior to the discussion of our modeling effort.

In order to simulate the deflagration-to-shock-to-detonation (DSDT) event occurring in a solid rocket motor without the destruction of full scale motor assemblies, several research groups [1-3] have studied the detonation transition present in a packed bed (10-20 cm in length) of granulated propellant/explosive. The detonation tube is closed at both ends and instrumented throughout to record stress levels and ignition front loci as the flame propagates from the igniter end, in some cases transitioning to a steady state detonation wave.

By analyzing the stress-time and ignition front data obtained in these types of experiments, the authors of Reference 1 have presented a scenerio of the events leading to the detonation transition. In brief, this includes the propagation of a weak compaction wave through the unreacted explosive due to the igniter blast, convective burning of the propellant particles, the buildup of a strong compaction wave due to the high pressure product gases and eventual shock initiation of the unreacted explosive upstream of the ignition front. The latter part of this proposed scheme of events is SDT (shock-to-detonation-transition), a well-studied method of initiating homogeneous and heterogeneous explosives without the use of a thermal ignition source. In SDT, the internal energy rise accompanying the shock front is sufficient to initiate chemical decomposition of the unreacted material.

In related experimental research, Pilcher, Beckstead, Christensen and King [4] investigated the effects of tube deformation on DSDT in porous beds of high energy solid rocket propellants (HMX-based). The research involved a series of ten DSDT experiments in addition to corresponding numerical predictions. HONDO [5], a dynamic structural analysis code provided by Sandia Laboratories was used in conjunction with the Krier/Van Tassell [6] two-phase flow code in order to couple flame spreading through the porous bed with the motor case deformation. For the material examined (HMX), confinement of the product gases was found to be important to DSDT outcome.

Experiments such as these provide useful information about the stress levels and detonation velocities obtained in DSDT events. However, in order to fully understand the physical mechanisms behind the shock formation and propagation into the porous material, one cannot rely on experiments alone.

The work to be presented in this paper represents an effort to analyze and numerically solve a mathematical model of the sequence of events observed in the experiments described above. It represents an important extension of research done earlier by Butler, Krier and Lembeck [7] on DSDT in HMX. The system of coupled partial differential equations describing the one-dimensional, two-phase reactive flow will be presented along with a finite difference technique used to numerically solve them. In addition to this, constitutive equations describing the states of the unreacted solid and gaseous products are also given.

Two distinct DSDT mechanisms will be discussed. The first is not a DSDT in the true sense of the word. That is, a steady state combustion wave, being fueled by the rapid burning of propellant grains, will propagatae through the granular bed and exhibit CJ detonation properties. However, because of the open pores and rapid decomposition of the solid grain, a shock wave does not propagate ahead of the detonation front as found in detonation waves travelling through homogeneous materials. The second DSDT mechanism does involve shock heating, but only after the granular bed has been compacted and the flow of hot gases has been terminated.

THE MODEL

The conservation equations (one-dimensional) describing the two-phase (solid-gas) flow of a reactive material consist of a system of six, nonlinear, coupled partial differential equations.

For the gas phase the conservation equations for mass, momentum and energy are expressed in the Eulerian form as

Gas Continuity

$$\frac{\partial \rho_1}{\partial t} = - \frac{\partial (\rho_1 u_g)}{\partial x} + \bar{S} \qquad (1)$$

Gas Momentum

$$\frac{\partial (\rho_1 u_g)}{\partial t} = - \frac{\partial (\rho_1 u_g^2)}{\partial x} - \frac{\partial P_g \phi}{\partial x} + \bar{M} \qquad (2)$$

Gas Energy

$$\frac{\partial (\rho_1 E_{gT})}{\partial t} = - \frac{\partial (\rho_1 u_g E_{gT} + \phi u_g P_g)}{\partial x} + \bar{E} \qquad (3)$$

and for the solid phase

Particle Continuity

$$\frac{\partial \rho_2}{\partial t} = - \frac{\partial (\rho_2 u_p)}{\partial x} + \bar{S} \qquad (4)$$

Particle Momentum

$$\frac{\partial (\rho_2 u_p)}{\partial t} = - \frac{\partial (\rho_2 u_p^2)}{\partial x} - \frac{\partial (1 - \phi) P_p}{\partial x} + \bar{M} \qquad (5)$$

Particle Energy

$$\frac{\partial (\rho_2 E_{pT})}{\partial t} = - \frac{\partial (\rho_2 u_p E_{pT} + (1 - \phi) u_p P_p)}{\partial x} + \bar{E} \qquad (6)$$

The terms S, M, and E represent the interphase mass, momentum and energy transfer terms given by

gas phase transfer terms

$$\bar{S} = \Gamma \qquad (7a)$$

$$\bar{M} = \Gamma u_p - \bar{D} \tag{7b}$$

$$\bar{E} = \Gamma(E_{chem} - u^2_p/2) - \bar{D}u_p - \dot{Q} \tag{7c}$$

solid phase transfer terms

$$\bar{S} = -\Gamma \tag{8a}$$

$$\bar{M} = \bar{D} - \Gamma u_p \tag{8b}$$

$$\bar{E} = \bar{D}u_p + \dot{Q} - \Gamma u^2_p/2 \tag{8c}$$

Here, the terms E_{gT} and E_{pT} represent the total (sum of kinetic and internal) energies in the gas and solid phases. The subscripts g and p denote gas and particle, respectively. In Eqs. (1)-(6), the phase densities ρ_1 and ρ_2 are defined as

$$\rho_1 = \rho_g\phi \quad \text{and} \quad \rho_2 = (1 - \phi)\rho_p$$

The variable ϕ represents the percent by volume occupied by the gas phase, $\phi = V_g/V_{total}$. The state equation for the gas phase is a nonideal Abel equation

$$P_g = \rho_g RT_g(1 + \eta'\rho_g) \tag{9}$$

where η' is a covolume term. For the solid phase we used a form of the Mie-Gruneisen equation.

$$P(v_s, e) = P_{HS}(v_s) + \frac{(e-e_{HS})\,\bar{\Gamma}\,(v_s)}{v_s} \tag{10}$$

In Equation (10), P_{HS} and e_{HS}, the Hugoniot pressure and Hugoniot energy, are used as the reference state and $\Gamma(v_s)$ is the Gruneisen coefficient representing the thermodynamic derivative,

$$\bar{\Gamma}\,(v_s) = v_s\,(\partial P/\partial e)_v \tag{11}$$

In Eqs. 7a-7c and 8a-8c the term Γ represents the rate of mass generation per unit volume per unit time and is given by

$$\Gamma = \frac{3}{r_p}(1 - \phi)\rho_p\dot{r}\,. \tag{12}$$

Here, r_p is the instantaneous particle radius and $\dot{r}$ is the surface burning rate specified as a function of pressure.

$$\dot{r} = bP^n, \tag{13}$$

where $\dot{r}$ has units of cm/sec. The term $\bar{D}$ is an interphase (gas-solid) viscous force

$$\bar{D} = \frac{u_g}{4r_p^2}\,(u_g - u_p)f_{pg}, \tag{14}$$

where f_{pg} is determined from drag experiments in packed beds. Finally, $\dot{Q}$ represents the interphase heat transfer rate

$$\dot{Q} = \frac{3}{r_p}\,(1 - \phi)h_{pg}(T_g - T_p). \tag{15}$$

In the analysis carried out here, the heat transfer coefficient was

$$h_{pg} = 0.65\left[\frac{k_g}{2r_p}\right][Re]^{0.7}(Pr)^{0.33} \tag{16}$$

NUMERICAL SOLUTION TECHNIQUE

The governing equations (Eqs. 1-6) discussed in the previous section are hyperbolic and highly nonlinear due to the chemical reaction terms. A method of lines technique [8] was implemented to solve the system of differential equations on a high

speed computer (Cyber-175). The technique requires that each spatial derivative in the equations be expressed as a second order (or higher) finite difference analog at each time level. The resulting set of ordinary differential equations (ODE's) are then marched in time by a standardized ODE solver. Because the resulting equations are very stiff, we chose to solve them using Gear's backward differentiation formulae (BDF) routine [9].

If one discretizes the propellant bed length into NN1 cells, the number of differential equations needed to be solved results in 6 x (NN1). Each of Eqs. 1-6 should be solved at each of the NN1 grid points for every time level. However, in a one-dimensional, one-directional wave propagation problem, some computational shortcuts can be taken. Since the wave motion initiates at one end, it is not necessary to solve the equations over the entire spatial domain. In order to minimize the computational time, we introduced a technique which computes the x-location of the lead compression wave after each time step. Any cell upstream of this point has yet to be disturbed by the flow field. Therefore, it is only necessary to integrate from x=0 up to and including the location of the lead wave. As a test, we solved a baseline case using both techniques. The first case solved all 6 x NN1 equations and the second solved only the "dynamic" domain. A RMS error evaluation of the pressure profiles at t = 10 usec gives an error of RMS = 3.2% between the two cases. The test case which solved the entire 6 x NN1 equations took 198 cpu seconds where the case which solved the "dynamic" domain only took 98 cpu seconds, a reduction of 50% in computer time.

RESULTS

As a baseline test case we chose to model a packed bed of granulated propellant, 20 cm in length and closed at both ends. The propellant/explosive was HMX (octogen) and was assumed to be consisting of unisized spheres. Nonspherical particles can easily be modeled by simply adjusting the sphericity factor, x/r_p in the decomposition rate ($\Gamma = (x/r_p)(\rho_2 \dot{r})$). For spheres, $x = 3$.

The initial conditions for this particular case include: porosity $\phi_0 = 0.30$, propellant particle size $r_{po} = 100$ μm, material density (HMX) $\rho_o = 1.90$ g/cc and initial temperature $T_o = 300$ K. The linear burning rate for the propellant particles is $\dot{r} = 2.54\ (.001\ P^{0.9})$ cm/s where P is the surrounding pressure measured in (psi). In order to start the transient combustion process, the material located at x = 0 is assumed to be ignited at t = 0. This initial configuration is typical of DSDT experiments run in the laboratory [2].

Figures 2-5 illustrate the profiles of various important parameters as time progresses and the combustion wave propagates through the material. Note that the pressure (Fig. 2), velocity (Fig. 3), and mass generation rate (Fig. 4) all asymptote to steady state values after approximately 80 usec. This occurs when the ignition front is located approximately 15-17 cm from the ignition source. This is typical of run-up lengths observed in actual DSDT experiments.

Figure 2 illustrates the pressure profiles obtained in the propellant bed at 2.5 usec increments. Because of the pressure scale, the plots for 0<t<20 usec have been excluded from this figure. The value of peak pressure is shown to approach 17 GPa in the steady state limit.

Once the steady state detonation wave has developed, the bed can be described as three distinct zones as is evident from all the figures. The region upstream of the shock front is undisturbed and remains at the initial thermodynamic state. At the shock/ignition front the propellant rapidly decomposes within a very thin zone of reaction. This is evident from the sharp spikes in the mass generation rate plots (Fig. 4). As in any steady state detonation wave, the rapid reactant → product transformation provides the necessary driving force for the steady state wave. Finally, downstream of the reaction zone is an all-gas expansion wave, extending back to a stationary zone of expanded product gases.

In Figure 5 the porosity, ϕ (gas volume/total volume) of the mixture is plotted as a function of x, the bed location. As the reaction front travels through the two-phase mixture, the solid reactants decompose and thus the value of ϕ increases until $\phi \to 1$ and an all-gas composition exists. An interesting observation made from the ϕ - x profiles is the compaction wave developed at the early times, $45 < t < 65$ usec. It will be shown later how this decrease in ϕ can effect the entire DSDT process. That is, under certain circumstances the value of ϕ may approach zero, indicating a complete blockage of the product gas flow.

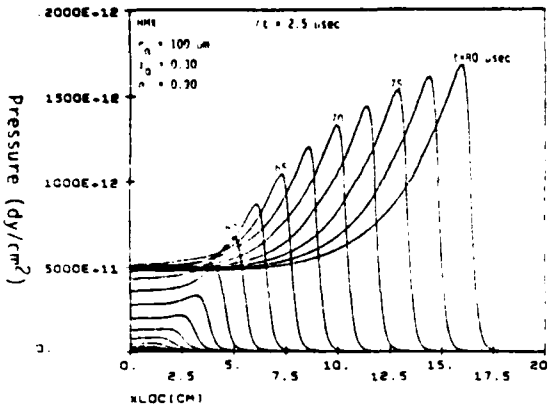

Fig. 2 Pressure-x profiles showing shock development and transition to steady state detonation.

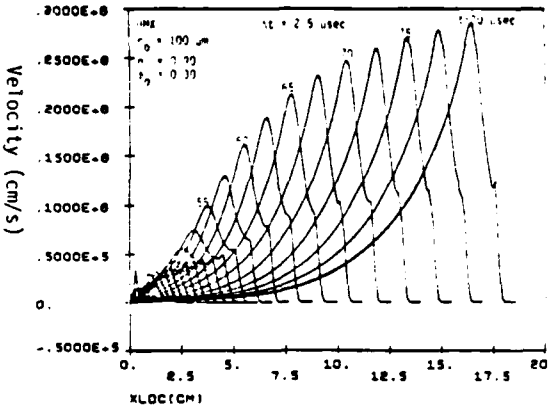

Fig. 3 Gas phase velocity profiles for same case as shown in Fig. 2.

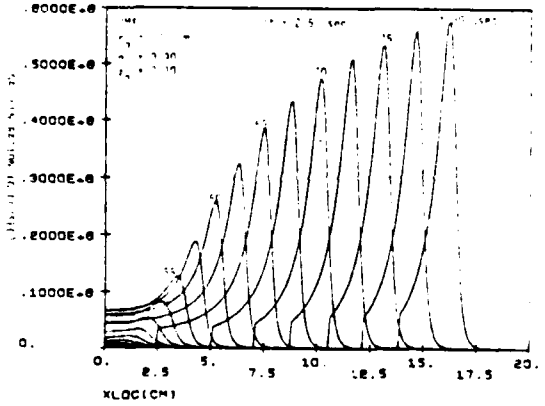

Fig. 4 Rate of gas generation from solid phase to product gas phase (Fig. 2).

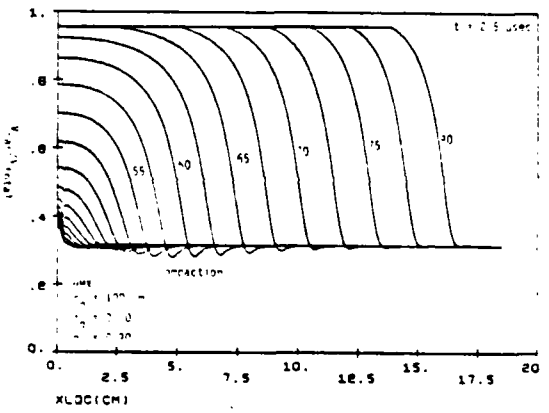

Fig. 5 Volume fraction of gas phase showing compaction in early times ($50 < t < 65$ μs).

Figures 2-5 show the ignition front to accelerate at first and then to stabilize at a detonation velocity D_{CJ} = 6.7 mm/μsec. The accompanying Chapman-Jouguet pressure is P_{CJ} = 17.0 GPa. These values are close in agreement with one-dimensional, planar detonation theory for granular explosives and with values obtained from TIGER predictions for HMX.

TIGER values for this case are

$$P_{CJ} = 17.3 \text{ GPa}$$

and

$$D_{CJ} = 7.05 \text{ mm/μsec}$$

The values of CJ pressure for various loading densities are shown in Fig. 6. Here, the loading density is defined as $\rho_0 = (1 - \phi)\rho_p$ where ρ_p is the crystalline density. Data for this plot were taken from TIGER predictions, Johansson [10], and the predictions made with our code. All three sources show detonation pressure to be a linear function of loading density squared.

Before proceeding with the discussion, some comments should be made regarding the general structure of the steady state wave solutions generated by our code. Unlike the classical ZND detonation wave, our results do not show shock compression

of the upstream reactants. In our results the reaction front and compression front appear to travel as one. This is due to the two-phase nature of the problem. When a detonation wave travels through a homogeneous material only stress waves can be propagated upstream of the reaction front. This, of course, neglects heat transfer by conduction which is of a lower order time scale than the detonation velocity. However, in a two-phase mechanical mixture both stress waves and hot product gases can propagate through the upstream material, thus changing the structure of the wave, and the detonation mechanisms.

In any case, the expansion wave following the steady state detonation should satisfy certain fundamental relations of fluid mechanics. In particular, any point along the expansion wave is related to the CJ point by [11].

$$P = P_{CJ}[1 + (\gamma-1)(u-u_{CJ})/2c_{CJ}]^{\frac{2\gamma}{(\gamma-1)}} \qquad (17)$$

where γ is the polytropic exponent, u is the particle velocity and c is the sound velocity. It is also known that the particle velocity must equal zero at the fixed boundary condition. Thus, the steady state pressure at the fixed wall should satisfy Eq. 17 with u = 0. For the case shown in Figs. 2-5, P_{wall} is calculated to be 4.6 GPa (46 kbar). This is consistent with the value predicted by the code, thus verifying that an actual steady detonation has been predicted.

A second observation made of the predicted results and consistent with theory is, $(dP/dt)_{x=0} \to 0$ once the steady wave has developed downstream. This indicates that the expansion wave reaches a zero velocity point somewhere between the detonation front and rear boundary and thus, the pressure at the rear boundary remains constant with time. It has been shown in the DDT calculations given in Ref. 7 that in some cases (moderate burning rate propellants) high pressures can be predicted, but a steady state detonation does not develop. (This is still a hazard in a solid rocket motor since the pressures attained well exceed the strength of the motor casing.) However, if the porous bed was ignited with the purpose of developing a certain strength shock, say to shock initiate a downstream solid charge [14], then the DSDT has failed, unless Equation (17) is satisfied.

PLUG FORMATION

In some instances the porosity upstream of the convective front may approach zero (100% solid). Our results show this to occur early in the process before the detonation wave develops. Also, it is more likely to occur when the propellant particles are large and slow burning initially. When this occurs the flow of hot product gases is restricted and thus, the upstream material can no longer be heated by convective means. The pore collapse and plug formation are illustrated in Fig. 7. Part A represents the initial configuration, just after ignition, and Part B illustrates the plug formation. Once the plug has formed, the material downstream of the plug is still reacting, acting as a driving force for the upstream matrix of material. This configuration is similar to DDT experiments performed on cast explosives [12] where one end is confined and end-burning initially. The result is coalescence of stress waves upstream of the reacting zone and eventual shock initiation.

Figure 8 is a plot of predicted ϕ - x profiles for a packed bed of HMX. The particles are spheres with a 200 μm diameter and the initial porosity is, ϕ = 0.32. The profiles are given at 2.5 μsec time increments. As shown in the figure, the porosity approaches ϕ = 0.10 at t = 75 μsec. At that time the plug was assumed formed.

The sequence of events occurring after a plug has formed are shown for a different case in Fig. 9. Here, the stress - x profiles are plotted as a function of $\bar{t}$, the time after plug formation. The compression wave generated from the reacting grains is reflected off of the plug and a strong shock wave is transmitted to the upstream material. Since the code does not yet have the capability to model the thermal explosion of a reactive material which has been shocked, one can only estimate a detonation run-up length from experimental Pop-plot data on similar materials. For example, for a shock wave of more than 1.0 GPa Dick [13] has shown the run-up length to be less than 0.5 cm for 1.24 g/cc HMX (ϕ_0 = .35).

CONCLUSIONS

The work discussed here addresses the problem of reactive, two-phase gas dynamics associated with the development of a detonation. It has been pointed out that as new, more energetic solid propellants are proposed for new propulsion systems the ability to understand the physics of this hazard become more necessary.

The research of flow simulation through modeling can give (and has provided) information that more clearly explains the transient events. Or, put more strongly, it would be virtually meaningless to attempt to understand DSDT by performing experiments alone, because it would be impossible to ascertain the flow coupling which provides the observed pressures and flame front.

We have shown two distinct ways in which a bed of granulated high energy propellant can detonate from a controlled deflagration. In both cases the bed is initially confined and has a high solids loading.

At first we showed that a bed of granular particles, very small in size (100 μm), can exhibit detonation characteristics by burning in a convective manner. Here, the important process was rapid gas generation from the burning particle. The detonation characteristics were also shown to match very closely those predicted by the TIGER code and experiment.

The second part of our proposed research in DSDT showed that if a plug ($\phi \to 0$) forms in the granular bed, prior to the rapid convective acceleration, the upstream plugged material can be shock loaded to strengths great enough to initiate detonation within a few millimeters.

In summary, the research shows a unique complex inter-coupling between propellant properties, (such as density, porosity, energy content, burning rate) and flow containment (such as permeability, convective heat transfer, and grain deformation) that occur in a DSDT event. A recent report by Baer and Nunziato [14] confirms that DSDT modeling of the type described herein can accurately model detonation experiments in porous reactive solids.

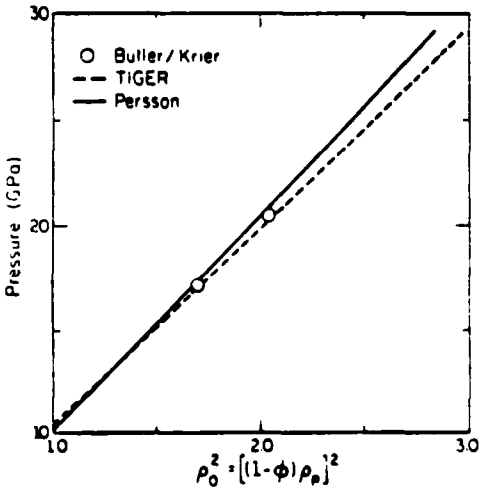

Fig. 6 Detonation pressure as a function of initial loading density squared for HMX.

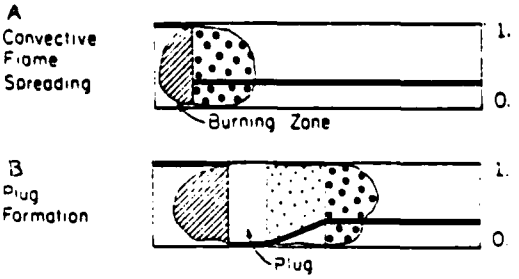

Fig. 7 Illustration of second branch of DSDT. Part A represents initial deflagration state. Part B shows the plug formation and upstream compaction.

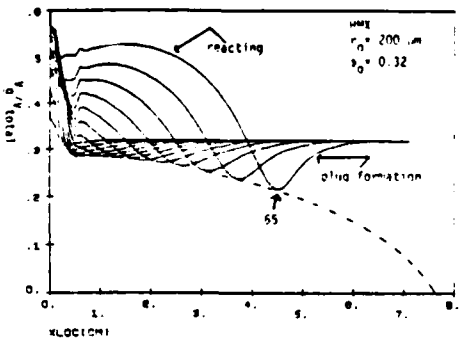

Fig. 8 Volume fraction of gas phase showing complete plug formation ($\phi \to 0$) for HMX, 200 μm.

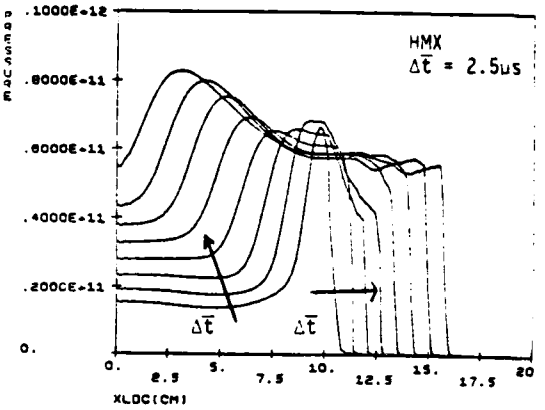

Fig. 9 Shock propagation upstream of plug after plug formation. The plug is formed around x = 10 cm.

REFERENCES

1. Bernecker, R. R., and D. Price, "Studies in the Transition from Deflagration to Detonation in Granular Explosives-I Experimental Arrangement and Behavior of Explosives Which Fail to Exhibit Detonation," Combustion and Flame 22, (1974), 111.

2. Bernecker, R. R., and D. Price, "Studies in the Transition from Deflagration to Detonation in Granular Explosives-II Transitional Characteristics and Mechanics Observed in 91/9 RDX/Wax," Combustion and Flame 22, (1974), 119.

3. Bernecker, R. R., and D. Price, "Studies in the Transition from Deflagration to Detonation in Granular Explosives-III Proposed Mechanism for Transition and Comparison with Other Proposals in the Literature," Combustion and Flame 22, (1974), 161-170.

4. Pilcher, D. T., M. W. Beckstead, L. W. Christensen, and A. J. King, "A Comparison of Model Predictions and Experimental Results of DDT Tests," Sixth Symposium on Detonation, White Oak, Maryland, Aug. 22-27, (1976), 258-266.

5. Key, S. W., Sandia Laboratories, Albuquerque, New Mexico, "HONDO-A Finite Element Computer Program for the Large Deformation Dynamic Response of Axisymmetric Solids," 1972, SLA-72-0039.

6. Krier, H., W. Van Tassell, S. Rajan, and J. T. Ver Shaw, IBL, BRL, APG, Md., "Model of Gun Propellant Flame Spreading and Combustion," March 1974, BRL Contract Report No. 147.

7. Butler, P. B., M. L. Lembeck, and H. Krier, "Modeling of Shock Development and Transition to Detonation Initiated by Burning in Porous Propellant Beds," Combustion and Flame 46, (1982), 75-93.

8. Hyman, J. M., "A Method of Lines Approach to the Numerical Solution of Conservation Laws," Third IMACS International Symposium on Computer Methods for Partial Differential Equations, June 20-22, 1979, Bethlehem, PA.

9. Gear, C. W., Numerical Initial Value Problems in Ordinary Differential Equations, Englewood Cliffs, New Jersey, Prentice-Hall Publishing Co., (1971).

10. Johansson, C. H. and P. A. Persson, Detonics of High Explosives, London, Academic Press, (1970).

11. Fickett, W. and W. C. Davis, Detonation, University of California Press, Berkeley, California (1979).

12. Macek, A., "Transition from Deflagration to Detonation," J. Chem. Phys., 31, (1959), 162-169.

13. Dick, J. J., "Measurement of the Shock Initiation Sensitivity of Low Density HMX," Combustion and Flame, 54, (1983), 121-129.

14. Baer, M. R. and J. W. Nunziato, "A Theory for Deflagration-to-Detonation Transition (DDT) in Granular Explosives," Sandia Report, SAND82-0293, (1983).

TABLE OF INPUT PARAMETERS

b	0.001 in/s $(psi)^n$
E_{chem}	6.2 MJ/kg
f_{pg}	$f_{pg} = ((1-\phi)/\phi)^2(276 + 5(Re/(1-\phi))^{.87}$ (Ref. 7)
c_{vg}	1.57×10^7 erg/g-K
c_{vp}	1.00×10^7 erg/g-K
n	0.90
Pr	0.72
r_o	100 - 200 μm
Γ_o	1.65
n'	4.00 cc/g
ϕ_o	0.30
μ_g	1.8×10^{-4} g/cm-s
L	20 cm
P_o	1.0×10^6 dynes/cm^2 = 1 kpa
ρ_{p_o}	1.9 g/cc
NN1	100 cells
T_o	300 K
ΔE_{ign}	5.0×10^7 erg/g

ACKNOWLEDGEMENTS

This work has been supported by the U. S. Air Force Office of Scientific Research under grant AFOSR 81-0145. Dr. Michael Stroscio was the program manager. The authors also wish to acknowledge the many helpful discussions on this problem with Dr. Jack Nunziato, Dr. Dennis Hayes, Dr. James Kennedy and Dr. Mel Baer, all from Sandia National Laboratories, Albuquerque, New Mexico.

APPENDIX B: Paper to be published in JANNAF Proceedings on Propulsion Systems Hazards (1984).

TRANSITION TO DETONATION FROM RAPID-COMPRESSION (RAMP-WAVES) GENERATED IN A BURNING POROUS BED

Christopher A. Cudak*, Herman Krier** and P. Barry Butler*
University of Illinois at Urbana-Champaign
Urbana, Illinois

ABSTRACT

Increasing the nitramine content of solid rocket propellants increases the overall performance of the system as well as the sensitivity to detonation by shock initiation. In some instances a confined zone of granulated propellant adjacent to a zone of cast propellant can provide a rapid enough pressure-rise rate to shock initiate the cast material. If the cast propellant is porous, the detonation will initiate at some location ahead of the granulated bed/cast material interface. The work presented here is an effort to numerically model this Deflagration to Shock to Detonation Transition (DSDT) event. Results will be presented showing the detonation build up for propellant beds with various initial configurations and boundary conditions.

LIST OF SYMBOLS

C_v	specific heat (erg/g/K)
e	specific internal energy (erg/g)
E_*	total energy (erg)
E^*	activation energy (erg/mole)
G	shear modulus (dynes/cm^2)
P_*	pressure (dynes/cm^2)
P^*	maximum axial stress (dy/cm^2)
Q	chemical energy release rate (erg/g/s)
R	gas constant (erg/g/K)
t_*	time (s)
t^*	characteristic rise time (s)
T_*	temperature (K)
T^*	characteristic burn temperature (K)
u	particle velocity (cm/s)
v	specific volume (cm^3/g)
V	volume (cm^3)
W	decomposed mass fraction
x	spatial location (cm)
Y	yield strength (dynes/cm^2)
Z	frequency factor (1/s)

Greek

α	$V_T/V_S = 1/(1_o - \phi)$
β	covolume (cm^3/g)
Γ	Gruneisen coefficient
ϕ	porosity, V_g/V_T
ρ	density (g/cm^3)
ψ	Helmholtz free energy (erg/g)

Subscripts

CJ	Chapman-Jouguet state
i	isentrope
g	gas
o	initial state
x	$\partial(\ )/\partial x$
s	solid
t	$\partial(\ )/\partial t$

INTRODUCTION

The probability of a detonation occurring in a solid propellant rocket motor greatly increases when secondary high-explosives are used as constituents in the propellant mixture. High-energy nitramines such as HMX (octogen) are often included in the propellant formulation in order to increase the specific impulse and thus overall performance of the rocket motor. However, when utilizing these high-energy formulations the hazard of a Deflagration to Shock to Detonation Transition (DSDT) becomes more likely. A DSDT event is defined as a controlled (subsonic) accelerating deflagration wave making a transition to a high order steady detonation wave. Once a region of granulated material has been ignited in a confined configuration, the DSDT can occur in the order of tens of microseconds and the result is total destruction of the rocket motor assembly.

Although little data is available on the actual DSDT process, most researchers agree that in order for DSDT to occur the rocket motor grain must first be damaged. Grain fragmentation can be the result of a handling accident, or case and/or nozzle failure during operation. The high surface-to-volume ratio fragments provide for the rapid pressurization rate necessary to shock initiate the remaining grain. Thus, by increasing the nitramine content of the propellant mixture the propensity to detonate is increased in two ways; the decomposition rate of the propellant increases and the shock sensitivity increases.

Approved for public release; distribution unlimited.

* Research Assistant, Department of Mechanical and Industrial Engineering
** Professor, Department of Mechanical and Industrial Engineering
* Research Assistant, Currently Assistant Professor, University of Iowa, Department of Mechanical Engineering
This work is supported by the Air Force Office of Scientific Research, Grant No. 81-0145.

In this paper we propose two possible methods in which DSDT can occur in a solid rocket motor. In the first case a section of the motor grain is completely fragmented, and in the second case, the grain is only partially fragmented. DSDT in a fully granulated bed (Case 1) was the topic of several research papers [1,2] by our group and will be discussed here only to provide a comparison with the second scenerio proposed. In Case 1, the transition to detonation occurs within the granulated material whereas in Case 2 it occurs in the upstream cast material. For the second scenerio the granulated zone is not long enough to DSDT, however, the nonfragmented material upstream can still detonate by shock initiation. In both cases, the confined burning of the propellant/explosive fragments is what drives the deflagration wave to detonation. The reader should consult Ref. 3 for a general overview of DSDT in different propellants and explosives and Refs. 4-5 for experimental results. Before presenting the analysis and modeling of the second case, a brief review of Case 1 is appropriate.

CASE 1

Begin by considering the rocket motor shown in Fig. 1. For illustration purposes we have selected a center-burning grain configuration. As far as we know, the propellant will not detonate unless a crack, filled with broken fragments, is developed in the cast grain [3]. That is to imply, the rapid pressurization necessary to shock initiate the cast propellant cannot be generated by extra "side-wall" surface burning (conductive combustion) alone. Therefore, to illustrate a DSDT event we have assumed there is a crack in the propellant and that within the crack we have assumed a packed bed of propellant fragments of known surface-to-volume ratio to exist. The fragment filled crack is enlarged and shown in Fig. 2. At some arbitrary initial time t_0, the bed is assumed burning at x = 0 (left-end in figure). Because of the assumed high surface-to-volume ratio of the confined sub-millimeter size particles, product gas generation increases beyond the level necessary for steady-state motor operation indicating that the amount of gas being generated by the decomposing propellant far exceeds the amount exiting the nozzle. Under these conditions, the crack in the motor can be modeled as a bed of granulated propellant confined on both ends (Fig. 2). As time progresses, pressure gradients are developed as a result of localized burning. Conserving momentum, the pressure gradients act to drive the hot product gases into the cracks and exposed pores between the propellant fragments. Convective heat transfer from the hot gas to the propellant surface will then ignite more of the particles, eventually leading to shock compression of the upstream propellant and subsequent detonation. Figure 3 shows a steady-state pressure profile some time after detonation. Ahead of the detonation wave are unreacted fragments of propellant. Within the detonation front the grains are rapidly consumed and to the downstream side of the wave

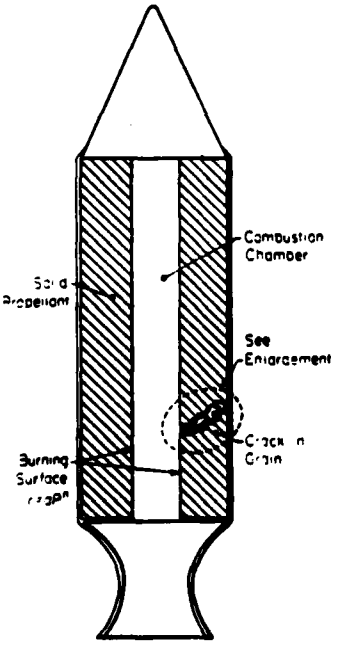

Fig. 1. Sketch of solid propellant rocket motor with cracked grain.

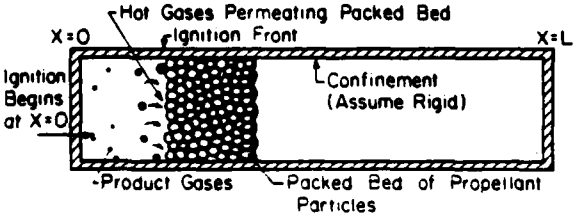

Fig. 2. Enlargement of granulated bed formed in rocket grain (See Fig. 1).

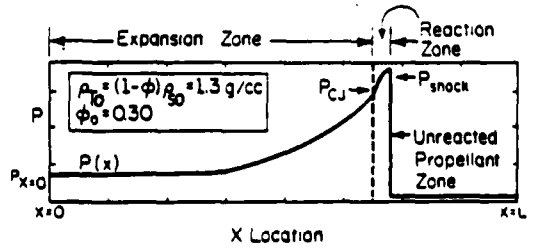

Fig. 3. Pressure-x profile of steady state detonation propagating into propellant bed.

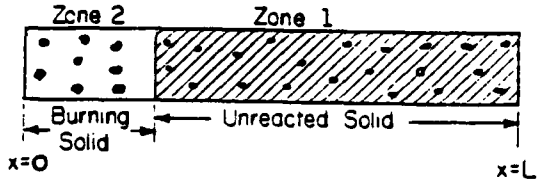

Fig. 4. Sketch of granulated bed/cast bed configuration (Case 2) for DSDT.

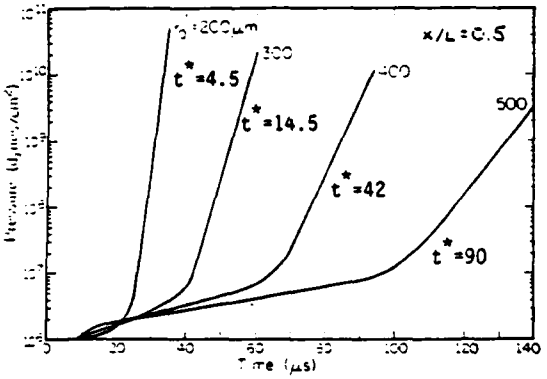

Fig. 6. Pressure-rise rates in granular bed of HMX (ϕ_0 = 0.3).

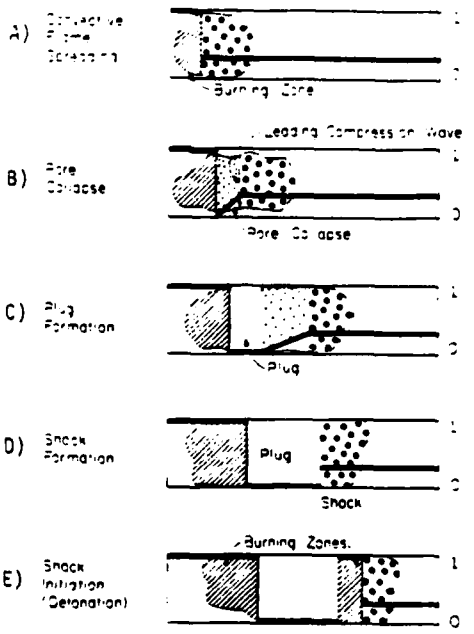

Fig. 5. Five-part sequence of events leading to DSDT.

the product gases expand in a Taylor expansion wave. This process is referred to by some as the accelerated convective burn model and is described in detail in the model developed by Butler, Lembeck and Krier [1].

CASE 2

A second DSDT scenerio involves a region of granulated propellant providing the impetus to shock initiate an adjacent region of cast explosive. This is illustrated in Fig. 4. The cast material (Zone 1) can contain 'blind' pores, but is assumed to be impermeable to the flow of hot gases from the granular zone (Zone 2). This implies that, unlike the first DSDT scenerio discussed, only stress waves can be transmitted across the Zone 1/Zone 2 interface. Figure 5 shows a schematic representation of the sequence of events leading to this type of DSDT. Superimposed on each section of the figure is a solid line representing the local gas porosity (volume of gas/total volume) as a function of x, the bed location. A value of ϕ equal to unity represents a zone of all gas while ϕ equal to zero indicates a homogeneous solid.

Part A shows a burning granular zone adjacent to a porous, cast explosive. Here, the heavy black dots are representative of microvoids in the cast material. Illustrated in Part B is the collapse of the pores, a result of the stress load transmitted across the granulated bed/cast explosive interface. Parts C and D show the length of the pore collapse zone to increase with time as the lead compression waves travel farther into the explosive. The finite compression waves coalesce into a shock front which then shock initiates the cast explosive downstream of the interface. From this location a detonation wave propagates through the porous material while a retonation wave propagates back through the compressed material (Part E).

In related research, Setchell [6] studied ramp-wave initiation mechanisms using waves with rise-times of 0.3 and 0.8 μs. In Ref. 6 the ramp-waves were developed by propagation of an impact-generated shock wave through a material which had the unique property of spreading out the shock front into a ramp-wave. In the work presented here, the rise-times were much longer, typically of the order of tens of microseconds. These slower rise-times are typical pressure-time histories generated within an accelerating deflagrating porous bed.

ANALYSIS OF DSDT IN A PARTIALLY GRANULATED BED

In a recent AGARD paper [2] we showed that under certain conditions, DSDT can occur in a granulated, porous bed of HMX (Case I scenerio). A few of the necessary conditions for DSDT to occur identified in Ref. 2 are: sufficient product gas confinement, a high initial loading density, a rapid gas generation rate, a bed length greater than the critical detonation run-up length and submillimeter sized particles. The steady state detonation solutions predicted in Ref. 2 were obtained by numerically solving the defining system of time-dependent conservation equations in conjunction with the proper constitutive relations. Values predicted for CJ pressure, CJ temperature, detonation velocity and detonation run-up length were in close agreement with values predicted by the thermoequilibrium code TIGER [7] and experimental data. The reader is referred to Ref. 2 for more on this subject.

The scope of the work presented in this paper is to model DSDT in the granulated bed/cast explosive configuration shown in Fig. 4. It is assumed that the granulated bed is not long enough to undergo DSDT, but by convective burning provides the driving force necessary to shock initiate the upstream cast explosive. For this analysis the cast explosive was assumed to have 'blind' pores and to be impermeable to the flow of product gases generated in the granular bed. This implies that only stress waves can be transmitted across the granular bed/cast explosive interface.

The first step to modeling DSDT in the Case 2 configuration is to determine the rate at which the reacting granulated bed stresses the cast explosive. This task was accomplished by running the DSDT code discussed in Ref. 2 for granular beds with lengths less than the detonation run-up length and recording the pressure-rise rate at the end opposite the igniter. Plotted in Fig. 6 are the P - t functions for propellant beds of various particle sizes. As shown in the figure, the pressurization rate in the granular bed, dP/dt, is strongly dependent on the size of the particles being consumed. The larger the particles being consumed, the slower the pressurization rate on the interface. Thus, from this type of analysis we have been able to determine the P(t) function used as a boundary condition for the stress wave analysis in the cast explosive upstream.

The P - t functions obtained from this modeling effort have been linearized and are expressed as

$$P(t) = (P^* - P_0)(t/t^*) + P_0 \qquad t \leq t^* \tag{1a}$$

$$P(t) = P^* \qquad t \geq t^* \tag{1b}$$

where P^* is the maximum stress in the bed. The parameter t^* is a characteristic rise-time for the ramp-wave input function.

GOVERNING EQUATIONS

The Lagrangian or material form of the governing equations are incorporated in the hydrodynamic analysis of a continuous material with a moving boundary. In the problem addressed, the moving boundary is a result of the applied stress load from the burning granulated bed. The one-dimensional unsteady form of the conservation of mass, momentum, and energy equations are expressed for the total mechanical mixture, as

$$v_t = v\, u_x \tag{2}$$

$$u_t = -v\, P_x \tag{3}$$

and

$$e_t = -P\, v_t + Q \quad . \tag{4}$$

In the above expressions v represents specific volume, u, particle velocity, e, the specific internal energy, P, the total stress, and Q the heat added per unit mass per unit time. The subscripts x and t indicate partial derivatives with respect to the Lagrangian spatial coordinate and time respectively. In addition to the conservation equations, a material equation of state, P = P(v,e), is needed in order to provide for mathematical closure.

For the solid material the equation of state $P_s(v_s,e_s)$ and the caloric equation $e_s(v_s,T_s)$ are expressed in terms of a Helmholtz free energy function [8], $\psi(v_s,T_s)$ and its thermodynamic derivatives through the Second Law of Thermodynamics reciprocity relations

$$P_s = -\frac{\partial \psi}{\partial v_s} \tag{5}$$

$$e_s = \psi - T_s \frac{\partial \psi}{\partial T_s} \tag{6}$$

With the assumption that the Gruneisen coefficient is constant, the Helmholtz free energy function takes the following form [8]

$$e(v_s,T_s) = J(v_s) + \Gamma C_{vs} \ln(v_o/v_s)(T_s - T_o) + C_{vs}[T_s \ln(T_o/T_s) + T_s - T_o] \quad (7)$$

where Γ is the Gruneisen coefficient defined by the thermodynamic derivative

$$\Gamma(v) = -v \left(\frac{\partial P}{\partial e}\right)_v \quad (8)$$

and C_{vs} is the specific heat at constant volume of the solid phase

$$C_{vs} = \left(\frac{\partial e}{\partial T}\right)_v \quad (9)$$

The term $J(v_s)$ in Eq. 7 is a nonlinear volume-dependent function determined from shock Hugoniot experiments [8].

With the introduction of product gases into the system, a constitutive law for the gas phase must also be provided. A nonideal covolume equation of state was chosen

$$P_g = \rho_g RT_g(1 + \beta\rho_g) \quad (10)$$

where R is the gas constant and β is a covolume correction term. The value of β is determined from the values for pressure, temperature and density at the CJ state predicted by the TIGER code. Table I gives a listing of those values for several loading densities of HMX. In accordance with the reciprocity relations defined earlier (Eqs. 5-6) the caloric equation of state for the gas phase is

$$e_g = C_{vg}(T_g - T_{go}) \quad (11)$$

where C_{vg} is the specific heat at constant volume of the product gases.

REACTIVE POROUS MATERIALS

The governing equations for conservation of mass, momentum and energy defined in the previous section (Eqs. 2-4) are expressed in terms of the thermodynamic properties (P,v,e) of the two-phase mixture as well as the dynamic variable u. Additional relations are needed to separate the individual phase properties from those of the mechanical mixture. It is assumed that any arbitrary volume V_T within the continuum can contain both solid and gas phases. Thus, the individual phase volumes sum to equal the total

$$V_T = V_g + V_s \qquad \text{or,} \quad v_T \equiv (1-w)v_g + Wv_s \quad (12a)$$

and, likewise for total energy E_T

$$E_T = E_g + E_s \qquad \text{or,} \quad e_T \equiv (1-W)e_g + We_s \quad (12b)$$

It is also assumed that $P = P_s = P_g$.

We define the material porosity as the ratio of total volume to volume occupied by the solid phase

$$\alpha = V_T/V_s \quad (13)$$

Initially, the volume not occupied by the solid material is assumed to be massless. By introducing porosity into the material, the mathematical description is not complete unless an additional independent equation is also provided.

Carroll and Holt [9] have performed extensive research in the area of mathematically modeling the collapse of a porous material under an applied external load. In their model the porous matrix is treated as a hollow sphere where the inner and outer radii are chosen such that pore size and overall porosity of the material are accurately represented. The assumed pore collapse occurs in three phases: (1) elastic phase, where the solid elastically deforms: (2) elastic-plastic phase, where plastic deformation begins at the inner radius and progresses outward until plastic deformation begins at the outer radius: and (3) plastic phase where plastic deformation occurs throughout. The $P - \alpha$ relations for the three phases of compaction and the appropriate range over which each applies are given by,

elastic phase $\quad \alpha_0 \geq \alpha > \alpha_1$

$$P = \frac{4G(\alpha_0 - \alpha)}{3\alpha(\alpha - 1)} \quad (14)$$

elastic-plastic phase $\quad \alpha_1 \geq \alpha > \alpha_2$

$$P = \frac{2}{3} Y \left[1 - \frac{2G}{Y x_1} x_0 - x + \ln \frac{2G x_0 - x}{Y x_1 - 1}\right] \qquad (15)$$

plastic phase $\qquad x_2 \geq x > 1$

$$P = \frac{2}{3} Y \ln \frac{x}{x - 1} \qquad (16)$$

where the limits between the three phases are given by

$$x_1 = \frac{2G x_0 + Y}{2G + Y} \qquad (17)$$

$$x_2 = \frac{2G x_0}{2G + Y} \qquad (18)$$

with Y and G the yield stress and shear modulus respectively. During pore-collapse, $P = P_s$.

THE COMBUSTION MODEL

A first order Arrhenius burn model is used to describe the chemical decomposition of the reactive material. It is given as

$$\frac{dW}{dt} = -ZW \exp\left(-E^*/\bar{R}T^*\right), \qquad \text{where, } W = m_s / m_{so} \qquad (19)$$

In the above equation W is the mass fraction of unreacted explosive, Z is the frequency factor, E^* is the activation energy, $\bar{R}$ the universal gas constant and T^* the characteristic burn temperature. During compression of the porous bed, T^* represents a "hot spot" temperature due to irreversible heating at pore sites. The localized hot spot temperature is different from the bulk shock temperatures and is calculated from a theory developed by Hayes [10].

The underlying assumption in this theory is that the shocked porous material is at one of two possible temperatures, a bulk shock temperature T, or a hot spot temperature T_H. The energy deposited by the shock wave is equated on a mass fraction basis to the sum of the reversible work done in isentropically compressing the bulk of the material, plus the irreversible heating of localized hot spots

$$\frac{P + P_o}{2} (v_{To} - v) = W_H\, e(v, T_H) + (1 - W_H)\, e_i\,(P). \qquad (20)$$

In Eq. 20 the left-hand side represents the total energy deposited in the material by the shock of strength P. The term $e_i(P)$ represents the energy required to isentropically compress the bulk of the material to the final shock pressure and the remaining energy term, $e(v,T_H)$, is the energy available to irreversibly heat the hot spots. The Hayes model assumes the mass fraction of the hot spots, W_H, to be equal to the preshock volume fraction of pores.

$$W_H = v_{To}/v_{so} - 1 \qquad = x_o - 1 \qquad (21)$$

Here, the subscript 'To' represents the initial porous state and the subscript 'so' refers to the homogeneous initial state.

TABLE I. EOS Parameters (P,T,v,e from THEOS)

x_o	ρ_{so} g/cc	P_{so} GPa	T_{so}(K)	v_{so} cc/g	D(mm/us)	B(cc/g)
1	1.90	16.67	3840	.4367	9.20	4.86
1.06	1.80	11.05	3973	.4260	8.77	4.60
1.12	1.70	13.60	4083	.4471	8.36	4.22
1.19	1.60	15.20	4171	.4707	7.98	4.03
1.27	1.50	22.22	4236	.4373	7.65	3.84
1.36	1.40	19.62	4280	.5276	7.33	3.74
1.45	1.30	17.26	4304	.5679	7.05	3.68
1.58	1.20	14.92	4337	.6064	6.76	3.61

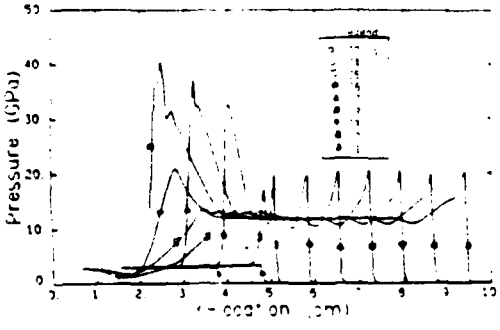

Fig. 7. A progress diagram for a stress wave propagating through a porous bed of HMX (x_o=1.3, ρ_{so}=1.4615), translating to a steady detonation and retonation (P*=3 GPa and t*=10 μsec).

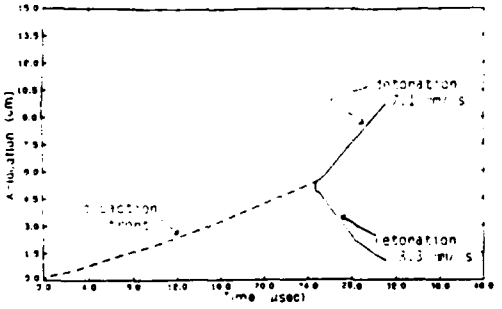

Fig. 8. Physical plane, showing locus compression, detonation and retonation fronts for DSDT event (γ=1.4615,P*=3GPa,t*=10μsec).

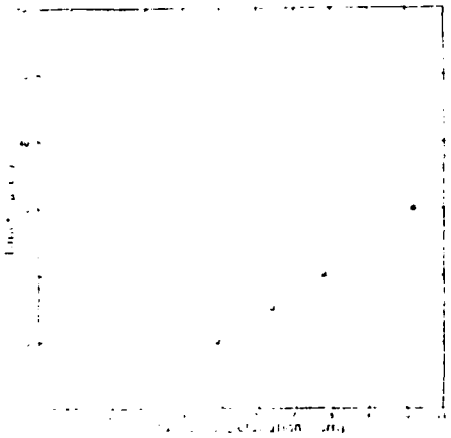

Fig. 9. An extrapolation for r_{cj} at t*=0μsec from calculated r_{cj} distances for various characteristic times (γ=1.4615).

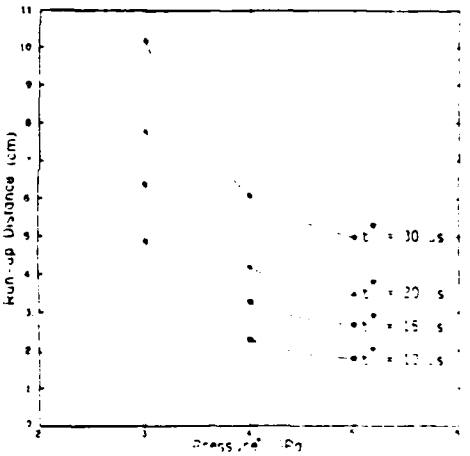

Fig. 10. A range of characteristic pressures and characteristic times plotted against the distance to detonation, r_{cj} (γ=1.4615).

NUMERICAL SOLUTION TECHNIQUE

Equations 2-19 completely define the fluid motion and thermodynamic state of a continuous, porous media. The system of equations were solved by using a finite difference numerical technique patterned after the WONDY code [11]. At t = 0 the bed of porous propellant/explosive is discretized into J cells labeled from left to right as j = 1, 2,. . . J. The thermodynamic properties pressure, temperature, internal energy and specific volume are assumed to be constant over the width of each cell. At the boundaries between the cells values for particle velocity and spatial location are assumed known. The reader is referred to Ref. 12 for a listing of the finite difference approximations to the governing differential equations and constitutive relations.

RESULTS

As stated earlier, the purpose of this work is to predict the transient events leading to detonation for a bed of porous, cast HMX being stress loaded at one end by a burning granulated bed of the same explosive. In our preliminary calculations we found that rise-times of 10 μs < t^* < 30 μs were typical of most of the granulated beds studied.

Figure 7 shows the stress-x profiles predicted at various times for a porous bed of HMX. This bed is ramp loaded at the left boundary to a maximum stress of 3.0 GPa and the characteristic rise-time in this case is $t^* = 10$ μs. As the left boundary is loaded, stress waves propagate through the porous material, collapsing the voids and coalescing into a shock front at approximately x = 5 cm. At the time, t = 24.7 μs, the irreversible heating of localized areas by the shock wave causes an explosion to occur. The rapid release of reactant chemical energy supports the detonation wave which propagates in the +x direction at a velocity of 7.1 mm/μs. At the same time, a backward traveling retonation propagates through the compressed material that remains between the detonation front and x = 0 boundary. This wave travels at a slightly greater velocity, 8.3 mm/μs than the detonation. This is expected since the material through which it is propagating is precompressed and therefore has a higher detonation velocity. The values predicted by our code for detonation velocity, D = 7.1 mm/μs, CJ pressure, P_{CJ} = 20.0 GPa and CJ temperature, T_{CJ} = 4500°K are in close agreement with values predicted by the thermochemical code TIGER (see Table I).

Moreover, the transition to detonation is delineated in Fig. 8. Here, the dashed line represents the stress wave propagating through the HMX, initiating the detonation at x = 4.87 cm. The solid lines represent the detonation front locus and retonation front locus. The discontinuity in slope at t = 24.7 μs indicates the time at which the tranistion occurs and the corresponding length is termed the detonation run-up length, ℓ_{CJ}. The discontinuity in the retonation front profile occurs when the wave interacts with the driving piston.

Experimental data are not available for 10-30 μs rise-time ramp-waves. Therefore, in order to validate our calculations, we have extrapolated our data in the 10-30 μs range back to a regime where data are available. Recall, Setchell [6] did experiments with $t^* = 0.8$ μs and Dick [13] has made run-up measurements for shock-to-detonation transition (SDT) in porous HMX (ρ_{To} = 1.24 g/cc). By extrapolating our $t^* - \ell_{CJ}$ data for ρ_{To} = 1.30 g/cc HMX (Fig. 9) down to $t^* = 0$ μs, a run-up length of ℓ_{CJ} = 5mm is predicted. Extrapolating the Pop-plot data in Ref. 13 gives a run-up length of ℓ_{CJ} = 3 mm.

Finally, a comparitive study was made for various ramp-wave rise-times and the results are shown in Fig. 10. Here, the material being stress loaded has the same initial conditions as the case studied in Fig. 7. The important point here is to compare the detonation run-up length, ℓ_{CJ}, for the various ramp waves. The longer the rise-time is, the greater is the run-up distance. This is an important point in rocket motor hazard analysis. The granulated bed/cast explosive configuration is representative of a rocket motor which has been partially fragmented. Even though the length of the fragmented propellant is not long enough to DSDT, the rapid rise-rate may shock initiate the intact propellant. However, if the distance needed to shock initiate the cast material is greater than any dimension of the rocket motor, DSDT is impossible. The motor will overpressurize and rupture, but it cannot detonate.

CONCLUSIONS

It has been shown by numerical simulation that under certain circumstances a porous, cast explosive will transition to a detonation when stress loaded in a ramp-wave fashion by an adjacent bed of granulated explosive. Rise-times for the waves studied ranged from 10 μs to 30 μs. In most cases, the bed detonated at some location downstream of the stress-loaded boundary and an energy sustaining retonation wave was shown traveling back towards the driving wall. The values predicted for the detonation properties were in agreement with TIGER data although the run-up lengths were much greater than any predicted for SDT experiments.

At the present time, the analysis is being applied to propellant beds with initial porosities, $1.05 < \alpha_o < 1.5$. In addition, the sensitivity of the ignition criterion to DSDT is being studied along with alternate chemical decomposition formulations (Eq. 19).

REFERENCES

1.) Butler, P. B., M. L. Lembeck, and H. Krier, "Modelling of Shock Development and Transition to Detonation Initiated by Burning in Porous Propellant Beds," Combustion and Flame 46, (1982), 75-93.

2.) Butler, P. B., and H. Krier, "Analysis of Deflagration to Shock to Detonation Transition (DSDT) in Porous Energetic Solid Propellants," AGARD Conference Preprint No. 367, paper No. 5, Lisse, The Netherlands, (1984).

3.) Bernecker, R. R., "The DDT Process for High Energy Propellants," AGARD Conference Preprint No. 367, paper No. 14, Lisse, The Netherlands, (1984).

4.) Price, D., and R. R. Bernecker, "Sensitivity of Porous Explosives to Transition from Deflagration to Detonation," Combustion and Flame 25, (1975), 91-100.

5.) Bernecker, R. R. and D. Price, "Studies in the Transition from Deflagration to Detonation in Granular Explosives. II. Transitional Characteristics and Mechanisms Observed in 91/9 RDX/wax," Combustion and Flame 22, (1974), 119-129.

6.) Setchell, R. E., "Effects of Precursor Waves in Shock Initiation of Granular Explosives," Combustion and Flame 54, (1983), 171-182.

7.) Coperthwaite, M. and W. H. Zwisler, "TIGER' Computer Code Documentation," Rept. PYV-1281, Stanford Research Institute, 1974.

8.) Baer, M. R., and J. W. Nunziato, "A Theory for Deflagration-to-Detonation Transition (DDT) in Granular Explosives," SAND Report, SAND82-0293, (1983).

9.) Carroll, M. M., and A. C. Holt, "Static and Dynamic Pore-Collapse Relations for Ductile Porous Materials," J. Appl. Physics, 43, No. 4, 1627-1636, (1972).

10.) Hayes, D. B., "Shock Induced Hot-Spot Formation and Subsequent Decomposition in Granular, Porous, Hexanitrostiblene Explosive," Detonation Physics Symposium, Minsk, Russia, 1981.

11.) Kipp, M. E., and R. J. Lawrence, "WONDY V - A One-dimensional Finite-Difference Wave Propagation Code," Sandia Report, SAND81-0930, (1982).

12.) Coyne, D. W., P. B. Butler, and H. Krier, "Shock Development From Compression Waves Due to Confined Burning in Porous Solid Propellants and Explosives," AIAA paper No. 83-0480, Reno, Nevada, (1983).

13.) Dick, J. J., "Measurement of the Shock Initiation Sensitivity of Low Density HMX," Combustion and Flame, 54, (1983), 121-129.

BLANK PAGE

END

FILMED

DTIC